Report No. K-TRAN: KU-13-6 ▪ FINAL REPORT ▪ January 2014

Wind Farm Turbulence Impacts on General Aviation Airports in Kansas

Thomas E. Mulinazzi, Ph.D., P.E., L.S.
Zhongquan Charlie Zheng, Ph.D.

The University of Kansas

A cooperative transportation research program between
Kansas Department of Transportation,
Kansas State University Transportation Center, and
The University of Kansas

Kansas
Department of Transportation

This page intentionally left blank.

1 Report No. K-TRAN: KU-13-6	**2 Government Accession No.**	**3 Recipient Catalog No.**
4 Title and Subtitle Wind Farm Turbulence Impacts on General Aviation Airports in Kansas		**5 Report Date** January 2014 **6 Performing Organization Code**
7 Author(s) Thomas E. Mulinazzi, Ph.D., P.E., L.S.; Zhongquan Charlie Zheng, Ph.D.		**8 Performing Organization Report No.**
9 Performing Organization Name and Address The University of Kansas Civil, Environmental & Architectural Engineering Department 1530 West 15th Street Lawrence, Kansas 66045-7609		**10 Work Unit No. (TRAIS)** **11 Contract or Grant No.** C1936
12 Sponsoring Agency Name and Address Kansas Department of Transportation Bureau of Research 2300 SW Van Buren Street Topeka, Kansas 66611-1195		**13 Type of Report and Period Covered** Final Report July 2010–June 2013 **14 Sponsoring Agency Code** RE-0605-01
15 Supplementary Notes For more information, write to address in block 9.		

16 Abstract

Wind turbines and wind farms have become popular in the State of Kansas. Some general aviation pilots have expressed a concern about the turbulence that the spinning blades are creating. If a wind farm is built near an airport, does this affect the operations in and out of that airport? Other problems associated with wind farms are their impact on agricultural aviation and their influence on radar detection of aircraft in the vicinity of a wind farm.

This research project has three objectives:

1. Determine the amount and pattern of the turbulence from a single wind turbine.
2. Determine the amount and pattern of wind turbulence from a wind farm, both in a horizontal direction and in a vertical direction.
3. This information will result in recommendations concerning the location of wind farms and their impacts of the safe operation of airports and other aviation activities.

The results of this project support the findings in the literature search that the turbulence from a wind turbine can impact operations at a general aviation airport. Two case studies were used to illustrate the impact of turbulence from a wind turbine on a general aviation airport. This project analyzed the roll hazard and the crosswind hazard resulting from a wind farm located near a general aviation airport. The wind turbine wake model is based on a theoretical helical vortex model and the decay rate is calculated following the aircraft wake decay rate in the atmosphere.

The roll hazard analysis showed that for the Rooks County Regional Airport, the potential roll hazard index is in the high range as far out as 2.84 miles. For the Pratt Regional Airport, the roll hazard index is in the high range as far out as 1.14 miles. These numbers are based on a gust wind of 40 mph that is below the turbine brake wind speed of 55 mph. As the results show, the scenario is different according to the relative locations and orientations of the airport and the nearby wind farm. Therefore, the analysis has to be performed for each specific regional airport.

The crosswind hazard analysis for the Rooks County Regional Airport showed part of the airport in the high range even under the mild wind condition at 10 mph. The wind turbine wake increases the crosswind component to more than 12 mph which is considered high risk crosswind for small general aviation aircraft. For the Pratt Regional Airport, the crosswind hazard is relatively small under the mild wind condition (10 mph). When there is a gust of 40 mph wind, the turbine wake induced crosswind puts the majority of runway areas to high hazard areas at both of the airports.

It is recommended that additional studies should be performed to draw the proper correlation between the hazard index developed in this study and the safe operation of aircraft at low airspeeds and at low flight altitudes operating near or at a general aviation airport.

17 Key Words Wind Turbine, Aviation, Airports		**18 Distribution Statement** No restrictions. This document is available to the public through the National Technical Information Service, Springfield, Virginia 22161	
19 Security Classification (of this report) Unclassified	**20 Security Classification (of this page)** Unclassified	**21 No. of pages** 61	**22 Price**

Form DOT F 1700.7 (8-72)

Wind Farm Turbulence Impacts on General Aviation Airports in Kansas

Final Report

Prepared by

Thomas E. Mulinazzi, Ph.D., P.E., L.S.
Zhongquan Charlie Zheng, Ph.D.
The University of Kansas

A Report on Research Sponsored by

THE KANSAS DEPARTMENT OF TRANSPORTATION
TOPEKA, KANSAS

and

THE UNIVERSITY OF KANSAS
LAWRENCE, KANSAS

January 2014

© Copyright 2014, **Kansas Department of Transportation**

PREFACE

The Kansas Department of Transportation's (KDOT) Kansas Transportation Research and New-Developments (K-TRAN) Research Program funded this research project. It is an ongoing, cooperative and comprehensive research program addressing transportation needs of the state of Kansas utilizing academic and research resources from KDOT, Kansas State University and the University of Kansas. Transportation professionals in KDOT and the universities jointly develop the projects included in the research program.

NOTICE

The authors and the state of Kansas do not endorse products or manufacturers. Trade and manufacturers names appear herein solely because they are considered essential to the object of this report.

This information is available in alternative accessible formats. To obtain an alternative format, contact the Office of Transportation Information, Kansas Department of Transportation, 700 SW Harrison, Topeka, Kansas 66603-3754 or phone (785) 296-3585 (Voice) (TDD).

DISCLAIMER

The contents of this report reflect the views of the authors who are responsible for the facts and accuracy of the data presented herein. The contents do not necessarily reflect the views or the policies of the state of Kansas. This report does not constitute a standard, specification or regulation.

Abstract

Wind turbines and wind farms have become popular in the State of Kansas. Some general aviation pilots have expressed a concern about the turbulence that the spinning blades are creating. If a wind farm is built near an airport, does this affect the operations in and out of that airport? Other problems associated with wind farms are their impact on agricultural aviation and their influence on radar detection of aircraft in the vicinity of a wind farm.

This research project has three objectives:

1. Determine the amount and pattern of the turbulence from a single wind turbine.
2. Determine the amount and pattern of wind turbulence from a wind farm, both in a horizontal direction and in a vertical direction.
3. This information will result in recommendations concerning the location of wind farms and their impacts of the safe operation of airports and other aviation activities.

The results of this project support the findings in the literature search that the turbulence from a wind turbine can impact operations at a general aviation airport. Two case studies were used to illustrate the impact of turbulence from a wind turbine on a general aviation airport. This project analyzed the roll hazard and the crosswind hazard resulting from a wind farm located near a general aviation airport. The wind turbine wake model is based on a theoretical helical vortex model and the decay rate is calculated following the aircraft wake decay rate in the atmosphere.

The roll hazard analysis showed that for the Rooks County Regional Airport, the potential roll hazard index is in the high range as far out as 2.84 miles. For the Pratt Regional Airport, the roll hazard index is in the high range as far out as 1.14 miles. These numbers are based on a gust wind of 40 mph that is below the turbine brake wind speed of 55 mph. As the results show, the scenario is different according to the relative locations and orientations of the airport and the nearby wind farm. Therefore, the analysis has to be performed for each specific regional airport.

The crosswind hazard analysis for the Rooks County Regional Airport showed part of the airport in the high range even under the mild wind condition at 10 mph. The wind turbine wake

increases the crosswind component to more than 12 mph which is considered high risk crosswind for small general aviation aircraft. For the Pratt Regional Airport, the crosswind hazard is relatively small under the mild wind condition (10 mph). When there is a gust of 40 mph wind, the turbine wake-induced crosswind puts the majority of runway areas to high hazard areas at both of the airports.

It is recommended that additional studies should be performed to draw the proper correlation between the hazard index developed in this study and the safe operation of aircraft at low airspeeds and at low flight altitudes operating near or at a general aviation airport.

Table of Contents

Abstract v
Table of Contents vii
List of Tables ix
List of Figures x
Chapter 1: Introduction 1
Chapter 2: Literature Search 3
2.1 Wind Turbine Specifications 3
2.2 Wind Terminology 4
2.3 Wind Farms and Aviation 4
2.3.1 Turbulence Impact Assessment 4
2.3.2 CAA Policy and Guidelines on Wind Turbines 5
2.3.3 Airport Cooperative Research Program Synthesis 28: Investigating Safety Impacts of Energy Technologies on Airports and Aviation 6
2.3.4 NationAir Aviation Insurance 6
2.3.5 Other Reports 7
2.4 General Aviation 8
2.4.1 Imaginary Surfaces of Airports 10
2.4.2 Operations at Airports 12
2.5 Wind Farms and the Environment, Health, Agriculture, and Economics 14
2.6 Conclusion of the Literature Search 18
Chapter 3: Wind Turbine Wake Hazard Analysis 19
3.1 Simulation of the Roll Hazard Caused by Wind Turbine Wake Helical Vortex 19
3.2 The Rooks County Case 20
3.2.1 The Roll Hazard Analysis 21
3.2.2 The Crosswind Hazard Analysis 23
3.3 The Pratt Regional Airport Case 26
3.3.1 The Roll Hazard Analysis 26
3.3.2 The Crosswind Hazard Analysis 28
Chapter 4: Conclusions and Recommendations 31
References 32

Appendix A: Wind Turbine Wake Vortex Circulation 35
Appendix B: Helical Vortex Model for Wind Turbine Vortex Wake 38
Appendix C: Rolling Moment Coefficient Calculation 39
Appendix D: Roll Hazard Index 43
Appendix E: Rolling Moment Coefficient Decay with Distance 45
Appendix F: Crosswind from Wind Turbine Wake on an Airplane 48

List of Tables

TABLE 2.1 Airport Reference Code for Maximum Crosswind 9

TABLE F.1 Possible Maximum Crosswind Velocity in the Wind Turbine Wake in Different Background Wind Speeds 49

List of Figures

FIGURE 1.1 Proposed and Existing Wind Projects in Kansas 1

FIGURE 2.1 Non-Towered Airport Approach Traffic Pattern 13

FIGURE 2.2 Map of Impact Risk per Unit Area for a Detached Blade 17

FIGURE 3.1 Wind Turbine Helical Vortex Model Used in the Case Analysis (with Color Representing the Velocity Magnitude) 20

FIGURE 3.2 Rooks County Regional Airport and Wind Farm with a Scenario of a Northwest Wind 21

FIGURE 3.3 (a) Rolling Moment Coefficient and (b) Hazard Index around the Rooks County Regional Airport 22

FIGURE 3.4 Approach Surface of Runway 18 in the Airport Layout Plan Drawing 22

FIGURE 3.5 Rolling Moment Distribution along the Approach Aurface of Runway 18 (All in the High Hazard Index Range) 23

FIGURE 3.6 Wind Farm with a Northwest Wind 24

FIGURE 3.7 Crosswind Speed and Hazard around the Rooks County Regional Airport 25

FIGURE 3.8 Pratt Regional Airport and Wind Farm with a Scenario of a Northwest Wind 26

FIGURE 3.9 (a) Rolling Moment Coefficient and (b) Hazard Index around the Pratt Regional Airport 26

FIGURE 3.10 Approach Surface of Runway 17 in the Airport Layout Plan Drawing 27

FIGURE 3.11 Rolling Moment Distribution along the Approach Surface of Runway 18 (All in the High Hazard Index Range) 28

FIGURE 3.12 Pratt Regional Airport and Wind Farm with a Scenario of a Northwest Wind 29

FIGURE 3.13 Crosswind Speed and Hazard around the Pratt Regional Airport 30

FIGURE A.1 Model of a Turbine in a Wind Tunnel Experiment 35

FIGURE A.2 Vorticity and Velocity Distribution 37

FIGURE D.1 Y-Direction Velocity on the Center X-Z Cutting Plane 43

FIGURE D.2 (a) The Rolling Momentum Coefficient in the Domain and (b) in the Zoom-In Domain 43

FIGURE E.1 Rolling Moment Coefficient Decay with Distance 46

FIGURE E.2 Rolling Moment Coefficient Decay with Distance 47

FIGURE F.1 45 Degree Direction Velocity Value from the Wind Turbine Wake on a Cutting Plane 48

FIGURE F.2 45 Degree Direction Velocity Value Added by the Background Velocity 48

Chapter 1: Introduction

Wind turbines and wind farms have become popular in the State of Kansas. Figure 1.1 shows the proposed and existing wind farm projects in Kansas as of February 2013. However, some general aviation pilots have expressed a concern about the turbulence that the spinning blades are creating. If a wind farm is built near an airport, does this affect the operations in and out of that airport? Other problems associated with wind farms are their impact on agricultural aviation and their influence on radar detection of aircraft in the vicinity of a wind farm.

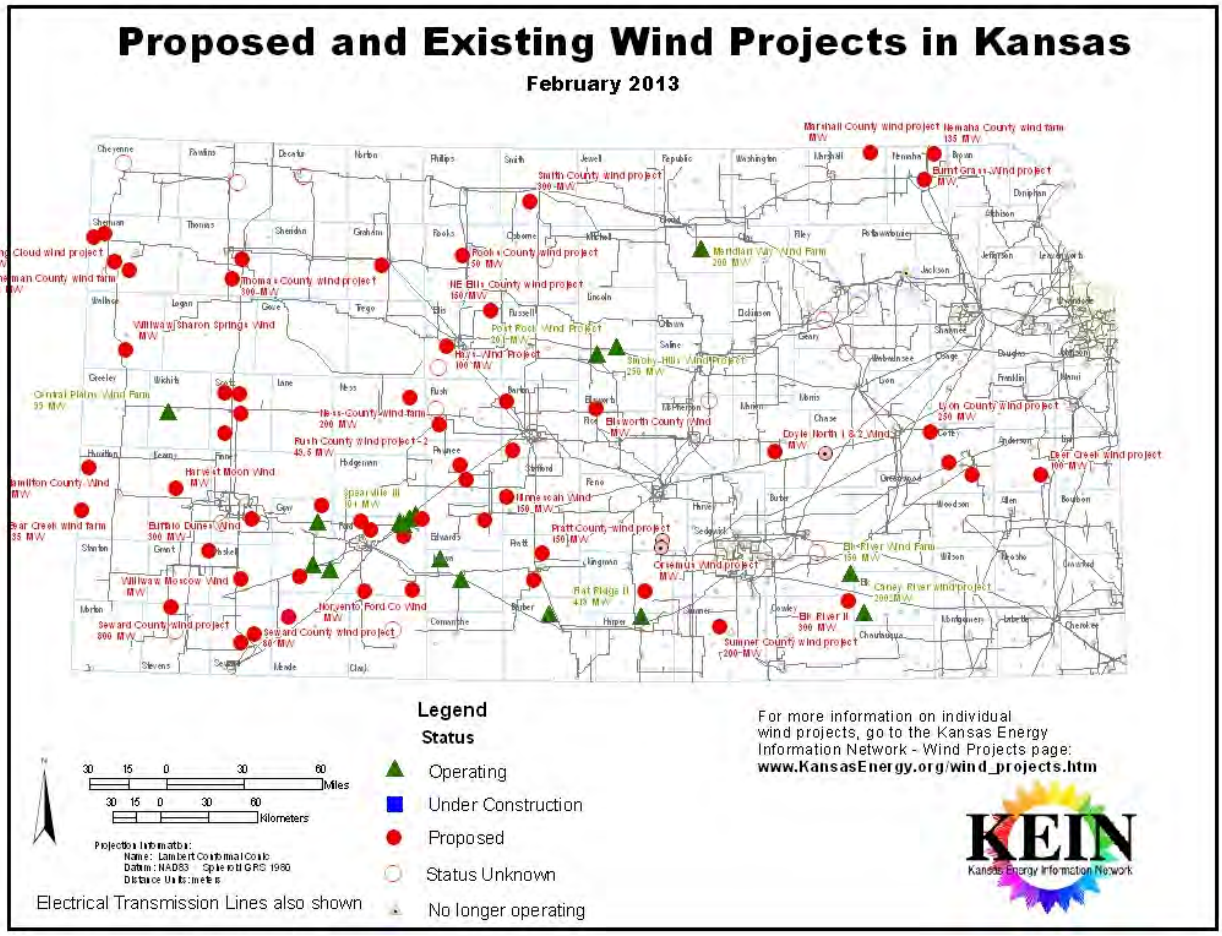

FIGURE 1.1
Proposed and Existing Wind Projects in Kansas

This research project has three objectives:

1. Determine the amount and pattern of the turbulence from a single wind turbine.

2. Determine the amount and pattern of wind turbulence from a wind farm, both in a horizontal direction and in a vertical direction.
3. This information will result in recommendations concerning the location of wind farms and their impacts of the safe operation of airports and other aviation activities.

There were five tasks in this project:

1. Determine the amount and pattern of the turbulence from a single wind turbine.
2. Determine the amount and pattern of wind turbulence from a wind farm.
3. Locate the existing and planned wind farms in the State of Kansas.
4. Locate the existing general aviation airports and their proximity to existing and proposed wind farms.
5. Write the final report

Chapter 2: Literature Search

2.1 Wind Turbine Specifications

After going through the popular wind turbine models of the top 10 wind turbine manufacturing companies in the world, the height of the wind turbine hub varied from 165ft to a maximum of 450ft. Many times the height of the hub is site specific, as it depends on the height at which the wind speed is the maximum. The rotor diameters vary from around 260ft to a maximum of 500ft, though the average diameter is around 300ft. The rated power of the wind turbines is between 8.0 MW to 0.6 MW (www.aweo.org/windmodels).

Johan Meyers (Katholieke Universiteit Leuven, Belgium) and Charles Meneveau (Johns Hopkins University) tried to find the optimal turbine spacing in a fully developed wind-farm. The researchers used the computational studies based on the Large Eddy Simulation, which allows them to predict the wind velocity at the hub height as a function of wind turbine spacing and loading factors. In this research, they used this simulation to predict the optimal spacing as a function of above parameters along with ratio of turbine costs to land surface costs. They found out that for realistic cost ratios the average optimal turbine spacing should be 15 times the diameter of the rotor as against the conventional 7 times. The above is true for large wind farms on flat terrain whose length exceeds the atmospheric boundary layer (height of approximately 1 km). The optimal spacing of wind turbines in small wind farms may depend on the location, as the turbines in the front will be operating under powerful winds compared to the one behind (Meyers and Meneveau 2012).

Ivan Mustakerov and Daniela Borissova studied the problems associated with optimal wind farm design in Bulgaria. The authors developed an optimization model for wind turbine type, number and placement based on given wind conditions and wind farm area being developed. To determine the optimization criteria they used wind farm investment cost and total power as functions of wind turbine type and number. The researchers considered two main wind directions regarding uniform and predominant wind directions for wind farm of shapes – square and rectangular. After testing a d eveloped wind farm numerically, they observed that the different practical requirements and restrictions define the different choices. Their results also confirmed that using big size turbines is more profitable than a large number of small size

turbines. The numerical tests show that the developed optimization approach can be applied to wind farm design (Mustakerov and Borissova 2009).

2.2 Wind Terminology

Start-up speed: Speed at which the rotor and blade assembly starts to rotate.

Cut-in speed: The minimum speed at which the wind turbine will generate usable power, generally between 7 and 10mph.

Rated speed: It is the minimum speed at which the wind turbine will generate its designated rated power. It is generally between 25 and 35mph for most of the turbines.

Cut-out speed: The speed at which the turbines stop generating power and shuts down, usually between 45 and 80mph (www.energybible.com 2012).

2.3 Wind Farms and Aviation

2.3.1 Turbulence Impact Assessment

EMD International A/S conducted a study on the turbulence impact from a wind farm located off shore. This study was undertaken because some sailors and recreational users off the coast of the island Hiiumaa complained about the turbulence. In this study the actual locations of the wind turbines were not considered, but a large number of turbines were selected. The turbulence was calculated to be 8m/s at a 10 m height on off shore locations. The size of the wind farm considered in this study was 636 MW, distributed on 212 uni ts. For calculations Vestas V90-3 was used, which has a nominal power of 3 MW, a rotor diameter of 90m and a hub height of 80m. The turbulence of wind was described by turbulence intensity, which is the ratio of wind speed changes to mean wind speed. Turbulence depends on t he terrain; sea surface causes little turbulence while forest area causes very high turbulence. The higher the turbulence, the longer is the distance required for dissipation. The wind turbines add wake to the wind turbulence. The wake can be recognized up t o 2000m (about 6600ft) downwind side of the turbine. The wake turbulence is the largest behind the turbine and decreases further downstream. The turbulence from turbines has a short and predictable spectral size unlike the natural turbulence. They concluded that the maximum turbulence from a single turbine is at 200m and is almost negligible after 500m. The researchers concluded that the turbulence impact of the

turbines is negligible beyond a few hundred meters, when compared with the turbulence on land (EMD International A/S 2010).

2.3.2 CAA Policy and Guidelines on Wind Turbines

The Civil Aviation Authority (CAA) in England is the statutory corporation which oversees and regulates all aspects of civil aviation in the United Kingdom (UK). The study focused on the issues related to the UK but lessons still can be applied here. There was also recognition in their report that both aviation and wind energy were important to natural interests and each side should cooperate to find solution to potential problems. The CAA published this document to give the aviation stakeholder a better understanding of the wind turbine related issues. In Chapter 2 of their report, they identified several impacts of wind farms on aviation. They report that Primary Surveillance Radar is adversely affected. If the wind turbine falls within the line of sight of the radar, then the radar misinterprets a wind turbine as an aircraft. Sometimes wind turbines cause a loss of sensitivity in detection of aircrafts to an extent that they are lost completely. The wind turbines form an obstruction and, thus, there is a region behind the turbine in which aircrafts are masked and cannot be detected. The receiver requires a large range to detect reflected signals from small and large aircrafts. If there is an obstacle such as a wind turbine, then it reflects a significant amount of signals and thus the receiver becomes saturated. The wind turbine also affects the Secondary Surveillance Radar even though it does not rely on the reflections from an object. The turbulence caused by the wake of the turbine extends downstream of the blades. The wake intensity depends on the size and height of turbines. It has been seen that the wind turbines create wake vortices similar to aircraft vortices, these can be hazardous to an aircraft. “Published research shows measurements at 16 rotor diameters, approximately 1500m (5000ft) downstream of the wind turbine indicating that turbulence effects are still noticeable.” The measurement of effect is very difficult even though modeling studies can predict the effects further downstream. The verification and validation processes of these models are still going on. They found that very light aircrafts such as gliders, gyroplanes, microlights, etc. are more susceptible to the wake turbulence. Thus, the CAA will analyze the

turbulence of wind farms near the airports on a case-by-case basis until they observe a significant pattern (Civil Aviation Authority 2011).

2.3.3 Airport Cooperative Research Program Synthesis 28: Investigating Safety Impacts of Energy Technologies on Airports and Aviation

This synthesis study was carried out to inform airport operators, aircraft pilots, airport planners and developers, legislators and regulators responsible for aviation safety of the visual and communications interference impacts of the new energy technologies on aviation. They list that the main concerns of using wind turbines are the height of the turbines and the communication system interference. In addition, the turbulence, lighting and marking of wind turbines are also a concern. Though CFR Part 77 deals with the height, size and location of aviation obstructions, this information is advisory in nature. Wind turbines are issued "No Hazard" determination if they are not located within the airport approach areas by the Federal Aviation Administration (FAA). Similar to the CAA findings, this report also states the adverse effects of wind turbines on the primary and secondary radars. They found that the turbulence from the wind turbines creates vortices at a distance of 2-6 rotor radii (250-750ft). Thus the aircrafts flying at a height of 200-400ft above ground, i.e. at the turbine level, are in danger. To minimize the effects of wind farms they have considered some mitigation options

- Appropriate siting to avoid communication system impacts.
- Re-route air traffic.
- Use of supplemental radars wherever the main radar is receiving false signals.
- Use radar absorbent materials on the turbines (Barret and Devita 2011).

2.3.4 NationAir Aviation Insurance

The NationAir Aviation Insurance (NAAI), an insurance company in Illinois, discussed the hazards of wind turbines to the aerial applicators. They say that the tax credits, and other grants and subsidies from the government drastically increased the number of wind turbines in the mid-west region. According to the NAAI Tower Policy all the recorded aerial applicator and tower collisions have been fatal. The wind turbine has hazards like wake turbulence and shadow flicker. The researchers found out that a typical commercial wind farm has 2.5 turbines per

square mile, with the exception of some states like Wisconsin, where there are 10-12 wind turbines per square mile. Turbine flickers can play visual “tricks” and lead to pilot disorientation. The specific location of wind farm can drastically impact application ability and its associated cost. The researchers also say that the MET (meteorological test towers) are very dangerous as they are below 200 feet and require no painting or marking. The NAAI has developed guidelines in order to inform the tower industry about the aerial applicators concerns, they are as follows:

- Construction Petitions should be provided to zoning authorities, landowners, applicators within a half mile from towers and regional agricultural aviation organizations.
- Towers should be avoided on prime agricultural land or locations which will inhibit spray.
- Information on whether the land will be or will not be suitable for aerial application after construction should be provided by the developers.
- The towers should be free standing without guy wires and in a linear pattern.
- Detailed field layout should be provided to those who work in the proximity after construction is completed. (NationAir Aviation Insurance 2012)

2.3.5 Other Reports

The De Kalb County, Indiana, case concerns the major safety of the MET towers set up to monitor the wind. The cost of aerial application increases with this and many operators refuse to operate within the confines of a wind farm. The farmers with land adjacent to a wind farm development are also affected. The operators charge 50% more than usual for aerial application in a wind farm zone. Potential impact on NexRad appears to be low, but one of the weather radars operating in Fort Wayne has seen impacts from towers in the Ohio counties of Paulding and Van Wert. The researcher concludes that the wind farm development will not affect aviation in all weather conditions but only in certain conditions. All the wind farm development should be studied on a case to case basis by a third party before local approvals are given. The researchers also state that the developments, which have been proven to not have any negative impacts, should not be restricted on unsubstantiated and unproven public claims. (Stump 2012)

The Fraunhofer Institute for Wind Energy and Energy System Technology (IWES) in Oldenburg, Germany developed a simulation which enables them to calculate the turbulence created by the wind farms, how they change the wind speed and how it affects the airplanes. The IWES conducted this research on behalf of BMR Windenergie, the operator of the wind farm, which has proposed a wind farm near an airfield. The researchers created a model of ground and wind profile of the area surrounding the proposed area of the wind farm. Over this model a grid was placed. The computer calculates the changes in the wind conditions and turbulence caused by the wind farms. Dr. Bernhard Stoevesandt said, "The true skill was creation of a grid: Because the points on the grid where the computer makes the individual calculations must lie exactly at the right place." Another challenge that the researcher faced was to depict the trail properly, which is the turbulence and wind conditions behind the rotor and determine its effects on aircraft. The researchers measured the trail at various individual points behind the rotor at actual wind farms in order to validate the simulations. The researchers carried out simulations for various wind directions, two different wind speeds and five different flight trajectories under which the airplanes will be influenced for varying lengths of time. The researchers found that the turbulence generated by the wind turbines is lower than the ordinary turbulence from the surrounding area. This finding can be applied to other airports to a limited extent, because of the fact that the surrounding terrain has a tremendous impact on the trail and, thus, it is very different for forested and hilly terrain compared to flat terrain (Stoevesandt 2012).

2.4 General Aviation

The FAA recommends a crosswind runway, if a runway orientation provides wind coverage less than 95% for any aircraft forecasted to use the airport on a regular basis. To calculate 95% wind coverage the crosswind should not exceed the following limits:

TABLE 2.1
Airport Reference Code for Maximum Crosswind

Airport Reference Code	Maximum Crosswind
A-I and B-I	12.10 mph
A-II and B-II	15 mph
A-III, B-III, and C-I through D-III	18.41 mph
A-IV through D-VI	23 mph

The Airport Reference Codes A-I or B-I are expected to accommodate single engine airplanes. Codes B-II or B-III refers to airports serving larger general aviation aircrafts and commuter type aircrafts. C-III is small or medium sized airports serving air carriers. And larger air carrier airports are with codes D-VI or D-V. (Federal Aviation Administration 2012)

Rate of change of wind speed and/or direction an aircraft experiences is called wind shear. There are two types of shear, namely vertical and horizontal, though generally they occur as a combination of both. Wind shear in aviation terms is defined as a sudden but sustained "variation in wind along the flight path of a pattern, intensity and duration that displaces the aircraft abruptly from its intended path so that substantial and timely control action is needed". Though wind shear is short lived it is probably the greatest hazard to aircrafts at low altitude. A substantial change in the lift generation linked with the aircraft inertia results in the displacement of the flight path. Terrain, constructed obstructions, thermals, and temperature inversions may cause wind shears. For a light aircraft, the closer to the surface a shear appears, the more dangerous it is. (Brandon 2012)

The Aircraft Owners and Pilots Association (AOPA) published two letters which state that "wind turbines have the potential to be a hazard to air navigation". "According to Greg Pecoraro, AOPA vice president of airports and state advocacy, it has become increasingly important for AOPA to educate lawmakers across the country about the effects of these systems on aviation, particularly so when the wind farms are in close proximity to airports. Aside from the obstruction itself, they can also interfere with communication and navigation, and wind patterns for all aircraft, especially gliders". Pecoraro went on to say, "If the systems (wind farms) were to be installed near arrival or departure paths of these facilities (airports), the safety of passengers and crew, as well as citizen below, would be greatly compromised" (Twombly 2009).

In an article titled, “Wind Farms Could be a Hazard to VFR Flights “ the AOPA is urging the FAA to find the 130 wind turbines proposed for the Nantucket Sound near Cotuit, Massachusetts, would pose a hazard to the many low-altitude VFR flights between the three area airports. The turbines could also disrupt local radar systems”. An AOPA Pilot Blog stated that “the National Weather Association newsletter had the statement that wind farms are showing up on NexRad radars. … They make radar returns that look a lot like a tornado vortex” (Namowitz 2012).

Another AOPA report has the title “Wind Farms Can’t Come at the Expense of Airports”. The mayor of Kentland, Indiana protected his town’s airport from a request by a local farmer to close the airport so he could build a wind turbine farm on his property” (AOPA 2010).

2.4.1 Imaginary Surfaces of Airports

To provide safe navigation of aircrafts to and from an airport, there are certain specifications to guard the airspace surrounding an airport. According to FAA, a runway protection zone should be provided at the end of a runway. It is an area on the ground beneath the approach surface, from the end of primary surface and extended to a point where the approach surface is 50ft above the primary surface. If the runway protection zone starts at any location 200ft beyond the end of the runway, then two protection zones are required, the approach protection zone and departure protection zone.

Part 77 of the Federal Aviation Regulations establishes standards to determine what would be considered as obstructions to the navigable airspace and sets requirements for notice to the FAA due to constructions and alterations; it also provides studies to explain the effects of obstructions on safe and efficient use of airspace. It is the responsibility of the airport operator to make sure that the aerial approaches to the airport are clear and protected and the land adjacent or in vicinity of the airport is restricted with measures such as zoning ordinances. Several imaginary surfaces have been established to determine whether an object is an obstruction to the airspace. These surfaces vary with the type of runway (e.g. utility, transport) and the approach planned for that runway (e.g. visual, non-precision instrument, etc.).

- Primary Surface: This surface is longitudinally centered on a runway. It extends 200ft from each end of the runway when the runway is paved; if the runway is unpaved it ends at the end of the runway. Its elevation is the same as that of the nearest point on the runway centerline.
- Horizontal Surface: This is a horizontal plane 150ft above the established airport elevation. The perimeter of this surface is constructed by swinging arcs of fixed radii from the end of the primary surfaces and the two arcs are joined by tangents.
- Conical Surface: It is a surface extending outwards and upwards from the periphery of horizontal surface at a slope of 20:1 for a horizontal distance of 4000ft.
- Approach Surface: This surface is longitudinally centered along the extended runway centerline. It extends outwards and upwards at a designated slope based on the type of approach planned or present.
- Transitional Surface: This surface extends outwards and upwards at right angles to the runway centerline and to the extended runway centerline at a slope of 7:1 from the sides of the primary surface up to horizontal surface and also from that of the approach surface. The width of the transitional surface is 5000ft from the edge of the approach surfaces.

Along with the above imaginary surfaces, existing or future objects are considered as obstructions if they are of greater height than any of following heights or obstructions:

- A height of 500ft above ground level at the site of the airport.
- A height of 200ft above ground level or above the established elevation of the airport, whichever is greater, within 3 nautical miles (3.45 miles) of the ARP (airport reference point) which has a longest runway of more than 3200ft. This is increased 100 ft for every mile up to 500 ft. at 6 miles from the ARP.
- A height within a terminal obstacle clearance area, including an initial approach segment, a departure area, and a circling approach area, that would result in the vertical distance between any point on the object and an established minimum instrument flight altitude in that area less than required obstacle clearance.

- A height that would increase the minimum obstacle clearance altitude within an obstacle clearance area along with turn and termination area on a federal airway or off-airway route.
- Any of the imaginary surfaces defined earlier. (Horonjeff, et al. 2010)

2.4.2 Operations at Airports

This is a standard operation procedure for an airport:

- First scan for traffic on the base and final approach legs. Turn on the landing and anti-collision lights, taxi on the runway and align with the runway centerline and take off.
- Departure Leg: Climb the extended runway centerline beyond departure end of runway up to 1000ft. Then look left and right to check for traffic conflict.
- Crosswind Leg: After climbing to the pattern altitude (1000ft) level off and reduce power. Go on crosswind for a half mile.
- Downwind Leg: Perform all the landing configuration tasks on this leg. Select a touchdown point on runway and descent when the spot is passed. Turn to base leg so as to achieve ½ - ¾ mile final approach leg.
- Base Leg: this leg is perpendicular to the runway. Scan for conflicting traffic on this leg. Approaching the turn point and scan for conflicts again.
- Final Approach Leg: Verify all the configurations. Keep scanning for traffic. Clear both sides of the final approach leg. (Air Safety Institute n.d.)

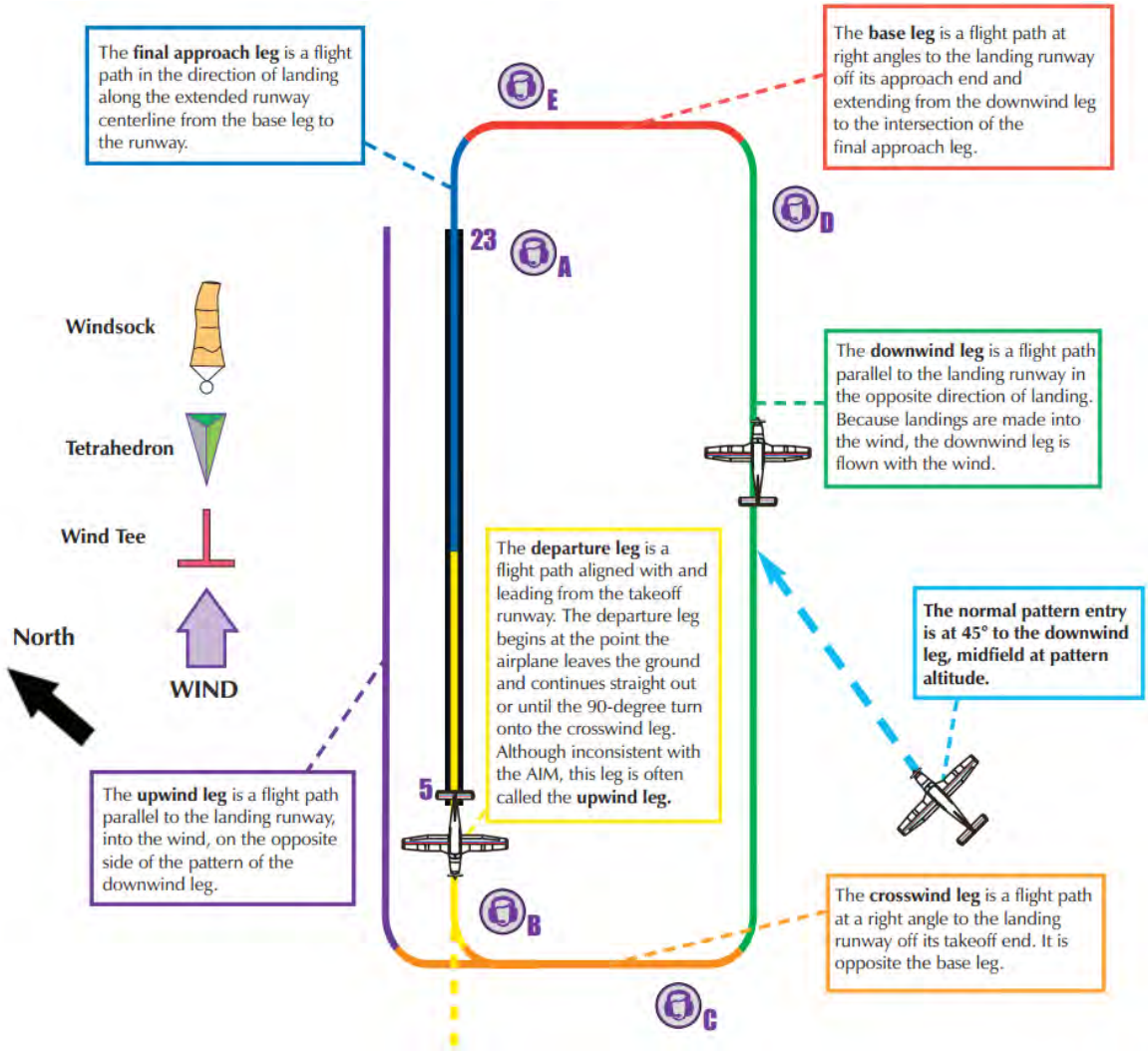

FIGURE 2.1
Non-Towered Airport Approach Traffic Pattern

Figure 2.1 illustrates the traffic pattern used when a p ilot approaches a non-towered airport. The location of a wind farm in relationship to an airport can impact the operations of the airport in three ways:

1. The wind turbines should not intersect any of the imaginary surfaces
2. The wind turbines should not be in the path of the recommended traffic pattern
3. The turbulence caused by the wind farm could impact airport operations even though the turbines don't violate 1 and 2 above.

2.5 Wind Farms and the Environment, Health, Agriculture, and Economics

The National Research Council studied the impacts of the wind farms on t he environment, aesthetics, cultural, recreational, social, and economics. The committee addressed the beneficial as well as harmful effects of wind farms. Though the committee studied the wind farms all over the US and world, their primary focus was on the wind farms located in the Mid-Atlantic Highland region. They concluded that wind farms had an adverse effect on ecology; birds and bat fatalities occurred due to collisions. They also observed that the new monopole turbines may have less fatalities compared to the older, lattice style turbines. They also observed that the bat fatalities were much higher compared to birds. They observed that the wind turbines had a great impact on the aesthetics of the area and this resulted in strong negative reactions. They suggest that the tools, which are available to study the project visibility and appearance as well as the landscape characteristics, should be used. Wind farms may have an impact on t he recreational, sacred and archeological sites as well, as natural scenery is part of recreation and, in the case of historic or sacred sites, their appreciation can be affected. The researchers do not have clarity to evaluate such situations and solve them. The noise from the rotor and flickering of the light due to the blades can cause irritation to the people living there. The noise can be monitored using various measurement techniques and the flickering of light has not been identified even as a mild annoyance, while in Europe it has been noted as a cause of concern. The wind turbine cause electromagnetic interference and has a potential to cause interference to television broadcasts. (National Research Council 2007)

Jay Calleja, Manager of Communications for National Agricultural Aviation Association, discusses the effects of wind energy on farming. The author states that when wind turbines are erected on the farm, aerial application becomes difficult. This is not only limited to the farm in which the turbines are installed, but the neighboring farms can also be affected. If the aerial aviators decide to apply on areas in or around wind turbines they will charge more. Apart from the fact that aerial application cannot be done, there is a deeper problem that exists and that being what the damage from the construction and maintenance does to the farm drainage systems. Although the wind companies do not say that they won’t repair the damage, the amount of money that the wind companies are obligated to pay may not match the amount that is required

to fix the farm drainage system. The author also gives many examples of how farmers have been affected even though they did not have wind turbines on their farms. Finally, the author concludes that the aerial applicators should educate farmers about the overall effect that wind turbine construction can have on farmlands and the ability to maximize production. (Calleja 2010)

Howard Graham studied the political and social controversy surrounding the proposed wind farm in the Flint Hills region, Kansas. The author states that even though most people of Kansas will back a wind farm project due to various reasons: they trust environmental groups, back local and state government and mistrust energy companies. Yet, in the case of Flint Hills, the Tallgrass Ranchers and Protect the Flint Hills and many environmental organizations urged the local and state authorities to ban wind turbines in Wabaunsee County, Kansas. This was done mainly based on the reason that the wind turbines will alter the social, cultural and aesthetics of the hills. All the new structures in the county require a permit. In this county "the establishment of land uses except agricultural and single-family uses" requires a conditional use. Also, the county limits the industrial structures to a maximum height of 45 feet along major roads and highways. So, the county law prohibits the industrial scale turbines in two ways: the height is more than the maximum and they cannot be erected on agricultural land as they are not permitted as a conditional use. The people residing in Flint Hills felt that erecting wind turbines was like driving a knife in their hearts. Thus, the county enacted a moratorium period of 2002-2013, during which the "County Zoning Administration shall not accept nor process applications for conditional use permits in connection with wind turbine electric generating project" till the moratorium was repealed or expired. (Graham 2008)

Michael C. Slattery, Eric Lantz and Becky L. Johnson estimates the economic impact of a 1398MW wind power development in four counties of west Texas using Job and Economics Development Impacts model. Impacts of projects are estimated at a local level (within 100 miles of the wind farm) as well as the state level. The researchers observed that during the four year construction phase almost 4100 full time equivalent jobs were created and out of these 58% were accounted for by the turbine and supply chain industry. The researchers found that, assuming 4 years of construction and a 20 year life of the wind farm, the total lifetime economic activity in

the state will amount to $1.8 billion, or $1.3 million per MW of installed capacity. The total economic activity at local level over the 20 year life cycle was substantial at $ 730 million, or $0.52 million per MW of installed capacity. The researchers conclude that, with this kind of impact observed from the wind industry and the potential to increase impacts by manufacturing equipment instate and developing trained wind industry labor, Texas appears to be well equipped to have increasing impacts from wind farm development. (Slattery, Lantz and Johnson 2011)

Johannes Pohl, Gundula Hubner, and Anja Mohs studied the stress effects of aircraft obstruction markings of wind turbines. The researchers state that along with the visual impact on the landscape, the stress effect of the aircraft markings is an emerging topic for resistance. As the height of the turbines increases, the number of markings increases as well. The researchers used environmental and stress methodologies to analyze the stress impact. The researchers sent out a questionnaire to 420 residents with a direct sight of 13 wind farms. They found that no substantial annoyance was caused by the obstruction markings. They also observed that the residents exposed to xenon lights reported intense and multifaceted stress compared to those exposed to LED lights. Also, the xenon lights negatively affected the general acceptance of wind farms. The residents also report more annoyance towards non-synchronized lights compared to synchronized conditions under certain weather conditions. Thus, the authors recommend that, to increase the social acceptance of wind farms, xenon lights should be banned, synchronized lights should be used and light intensity should be adjusted. (Pohl, Hubner and Mohs 2012)

Giuseppe Carbone and Luciano Afferrante defined the setback distance and/or buffer zones to reduce the risk of damage or injury from rotor failure. Currently, the distances are based as a "Rule of Thumb" based on the height of the tower and are often overestimated. The researchers combined a 3D dynamic model of detached blade fragment with a rigorous probabilistic approach. Their results show that there are large portions which are safe, even though they are located within the maximum range of the detached blade. Figure 2.2 below shows the safe and unsafe zones around a wind turbine (Carbone and Afferrante 2013).

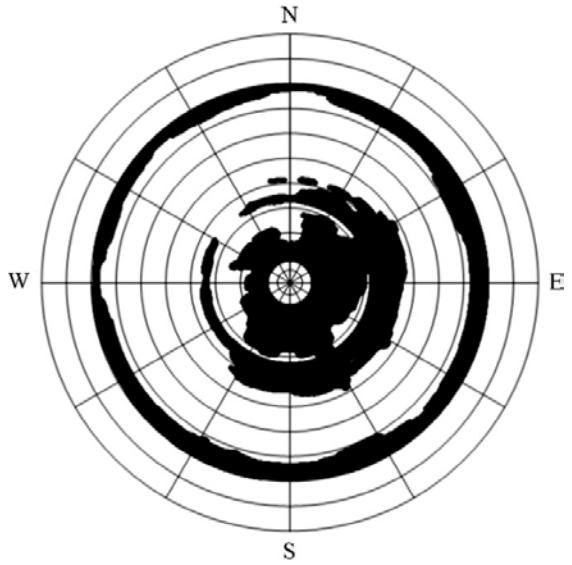

The external circle has a radius of 200 m and the radial distance between the two contiguous circles is 20 m. White areas are the safe regions.

FIGURE 2.2
Map of Impact Risk per Unit Area for a Detached Blade

Loren D. Knopper and Christopher A. Ollson reviewed the literature on the health effects of wind turbines and compared the peer-reviewed and popular literature. They searched for literature from the Thomas Reuters Web of Knowledge and Google. They concluded that the peer-reviewed differed from the popular literature in some ways. The reviewers found that the peer-reviewed studies the turbine annoyance was attributed to turbine noise, but were, in fact, strongly related to visual impact, attitude towards turbines and noise. The peer-reviewed articles only report health effects due to environmental stress that lead to annoyed/stressed state and does not demonstrate a link between physiological health effects of the people living close to the turbines and noise they emit. While on the other hand, they observed in popular literature that the health effects are related to the distances from the turbines. In conclusion, they observed that both type of studies had a common conclusion that being that the noise from turbine leads to annoyance to some people. They concluded that the change in the environment cause health effects and not the turbine specific variables like audible noise (Knopper and Ollson 2011).

2.6 Conclusion of the Literature Search

There is a need for more detailed information on the impact of the turbulence resulting from wind farms on a general aviation airport. The wind turbulence from a single wind turbine was simulated in the project and the methodology is presented in the next chapter of this report.

Chapter 3: Wind Turbine Wake Hazard Analysis

The potential hazard caused by wind turbine vortex wakes can be viewed as two different types: the induced roll hazard on the aircraft and the gusty crosswind from the vortex. Therefore, the wind turbine wake hazard is analyzed based on two criteria: *the roll hazard criterion and the crosswind hazard criterion*.

In the following analysis, we investigated two cases, the Rooks County Regional Airport and the Pratt Regional Airport. In each case, the potential roll and crosswind hazard range caused by the proposed nearby wind farm were studied.

The case study conditions are assumed as (www.aweo.org/windmodels):

- Wind turbine center height: h = 400 ft
- Turbine blade diameter: D = 300 ft
- Typical GA airplane wing span: L = 30 ft
- Atmospheric wind speed range: v = 10mph-40mph

3.1 Simulation of the Roll Hazard Caused by Wind Turbine Wake Helical Vortex

Under the situation of the highest wind speed V = 40 mph (58.67 ft/s), the circulation of the wind turbine wake helical vortex is $\Gamma = 5006.3$ (ft^2/s), which is calculated based on the model in Appendix A. Using this circulation value, a single turbine wake helical vortex was simulated. Figure 3.1 shows the simulated turbine wake helical vortex. The mathematical model is presented in Appendix B. The color represents the velocity magnitude.

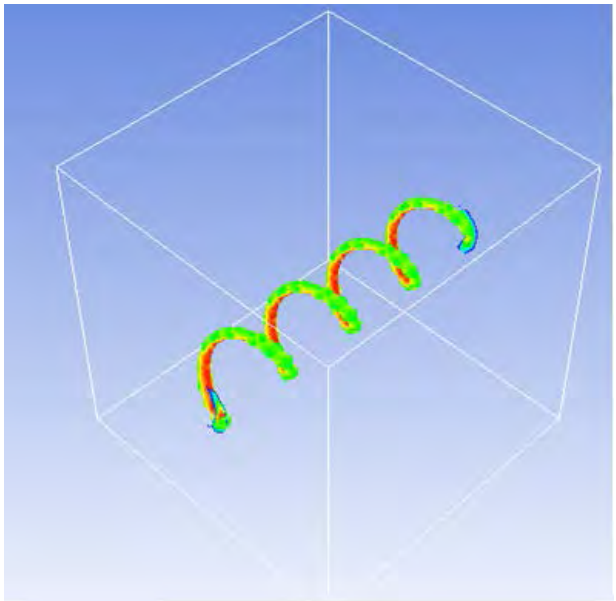

FIGURE 3.1
Wind Turbine Helical Vortex Model Used in the Case Analysis (with Color Representing the Velocity Magnitude)

Using the velocity field, the rolling moment coefficient acting on an airplane could be calculated (Appendix C). The hazard index range for the wind turbine induced rolling moment coefficient was defined as:

- Above an induced rolling moment coefficient of 0.28: high hazard
- Between 0.1 to 0.28: medium hazard
- And below 0.1: low hazard.

Please refer to the Appendix D to see how to determine these values.

3.2 The Rooks County Case

Figure 3.2 shows the aerial image and a sketch of the Rooks County Regional Airport. Runway 18-36 is the only existing runway in the center of the airport.

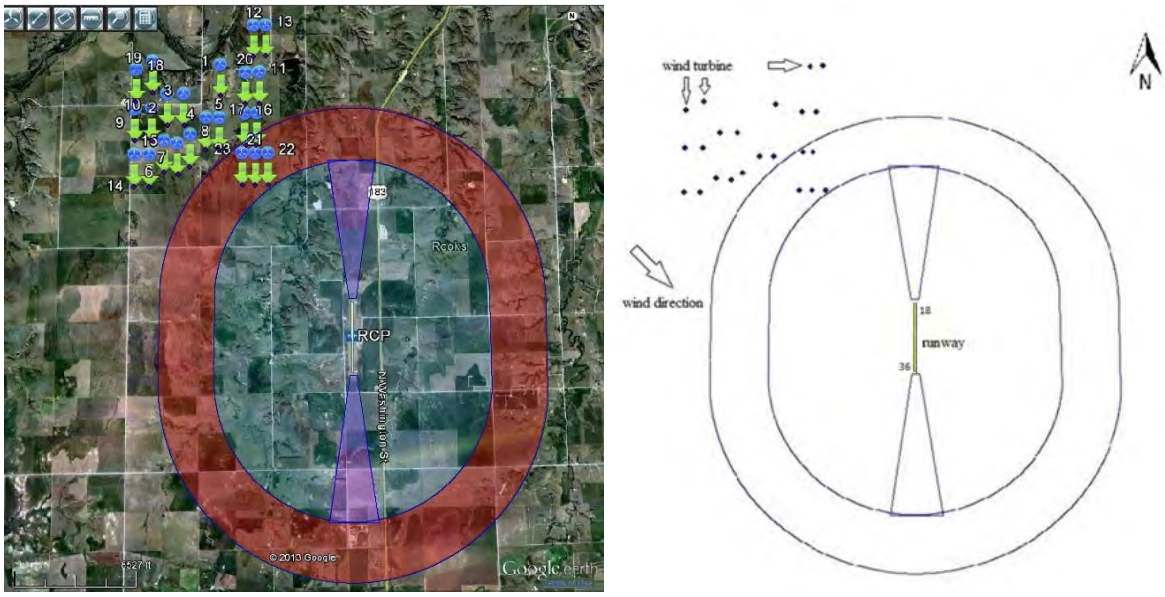

FIGURE 3.2
Rooks County Regional Airport and Wind Farm with a Scenario of a Northwest Wind

3.2.1 The Roll Hazard Analysis

Based on t his decay distribution in Appendix E, the induced rolling momentum coefficient due to the wind turbine wake on the encountering aircraft, and the hazard index near the runway, can be calculated. The contours for Runway 18-36 under the 40 m ph (which is assumed to be the highest possible safe wind speed under which wind turbines can operate) wind speed condition are shown in Figure 3.3. The rhombus area in Figure 3.3a is a cross section of the area where the helical vortex exists (between two red lines) and the area near the runway from south to north (between the two green lines). Figure 3.3b shows the exact rolling moment value in the area and Figure 3.3b shows the hazard index. As Figure 3.3b shows, the area around the runway is within the high hazard region (determined in 3.1).

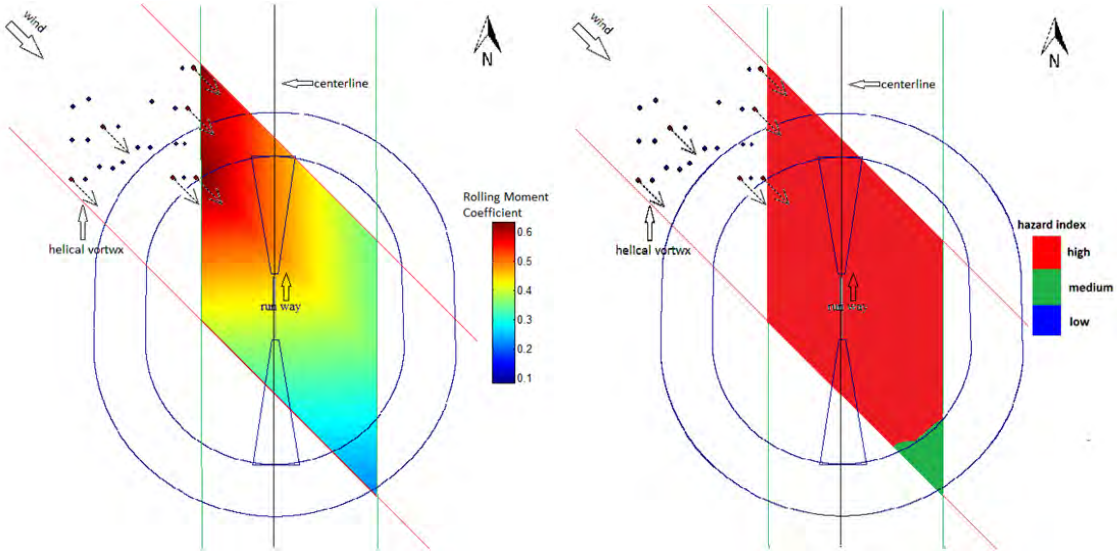

FIGURE 3.3
(a) Rolling Moment Coefficient and (b) Hazard Index around the Rooks County Regional Airport

Figure 3.4 is a plot of the end of Runway 18 and its approach surface from the airport layout plan drawing provided by the Kansas Department of Transportation. There are two approach surfaces: one is 20:1 approach surface and the other is 34:1 approach surface.

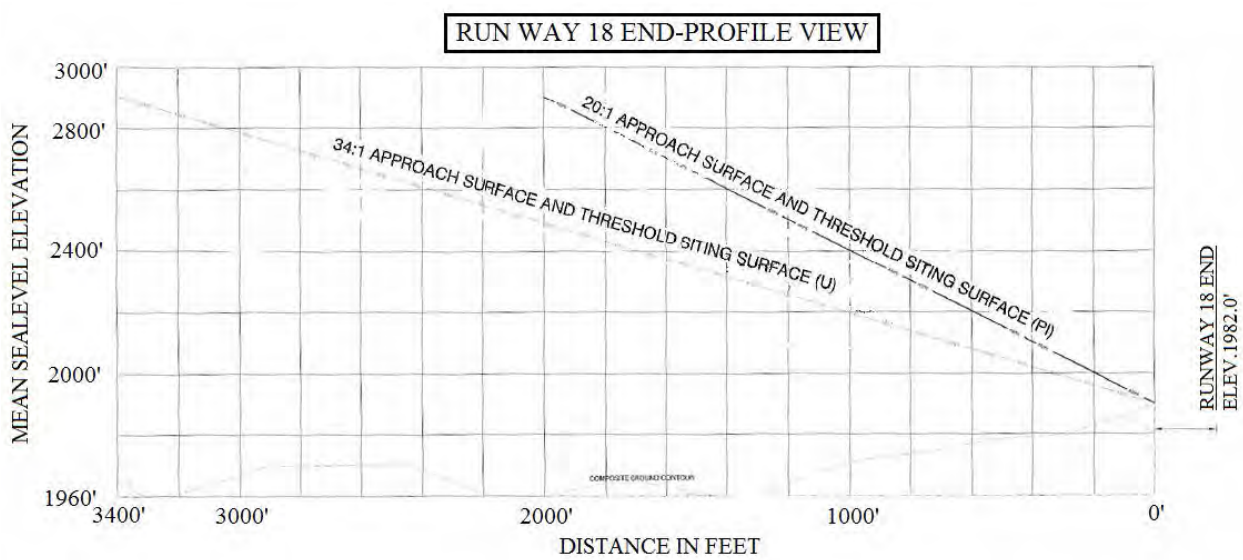

FIGURE 3.4
Approach Surface of Runway 18 in the Airport Layout Plan Drawing

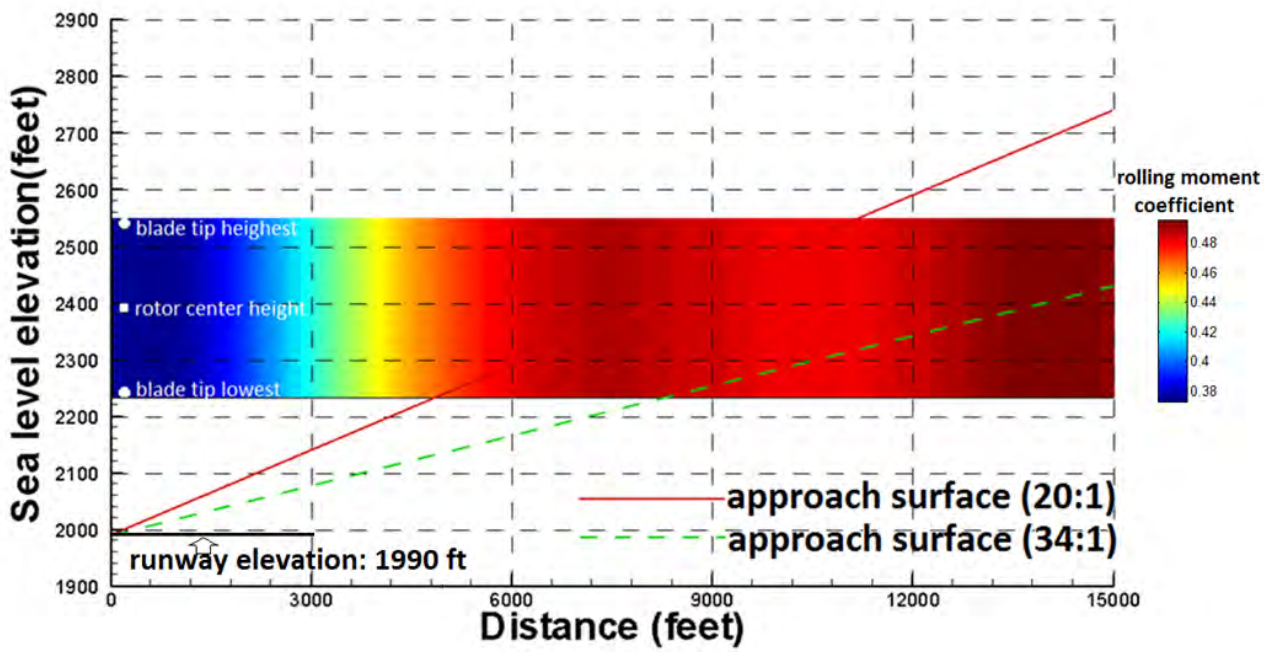

FIGURE 3.5
Rolling Moment Distribution along the Approach Aurface of Runway 18 (All in the High Hazard Index Range)

The approach surface portion in the above plot is about 100 ft. Since the turbine tower center is 400-foot high, we extended the plot following the trend and put the contours of the rolling moment coefficient in Figure 3.5 for the elevation between 2240 ft (the lowest blade tip elevation) and 2540 ft (the highest blade tip elevation). The rolling moment coefficient along this runway and the extended trend up to 15000 ft distance is always in the high hazard range. But for the approach surfaces, only within the height between two tips the airplane will experience the high hazard.

3.2.2 The Crosswind Hazard Analysis

Under the situation of the highest wind speed v = 40 mph (58.67 ft/s), the circulation of the wind turbine wake helical vortex is Γ = 5006.3 (ft^2/s). Using this circulation value, we simulated a single turbine wake helical vortex, as Figure 3.1 shows. In aviation, a crosswind is the component of wind that is blowing across the runway making landings and take-offs more difficult. Because the helical vortex can also enhance the crosswind, we need to assess the crosswind hazard in the area around the runway.

Figure 3.6 shows the aerial image and a sketch of the Rooks County Regional Airport. The wind direction is northwest. So as a component of it, the crosswind direction to Runway 18-36 is from west to east.

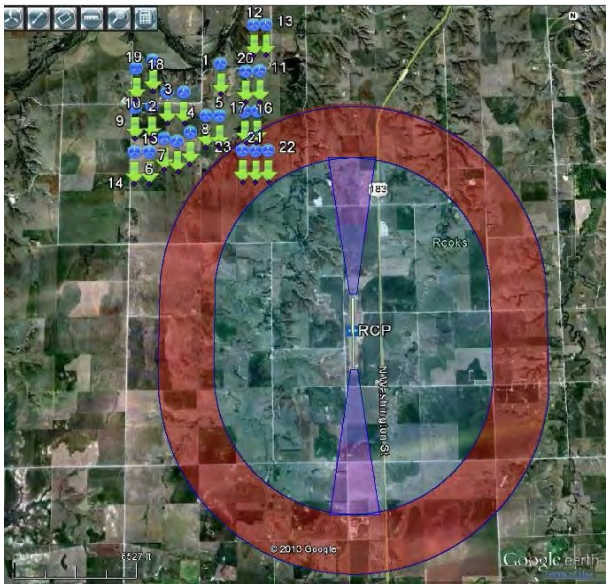

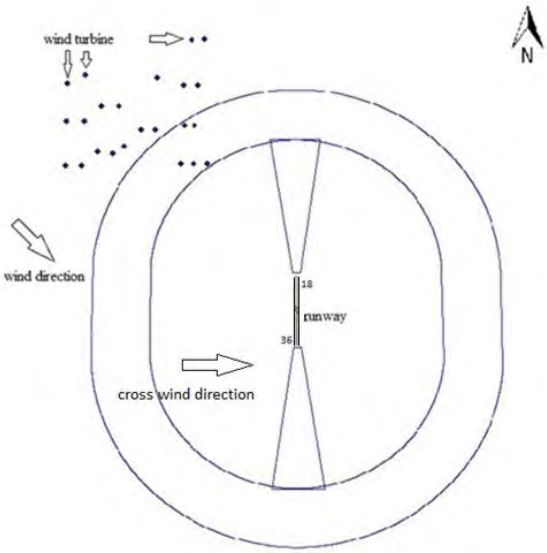

FIGURE 3.6
Wind Farm with a Northwest Wind

Based on the same decay distribution in Appendix E, the crosswind speed and the hazard index near the runway can be calculated (see Appendix F).

If there is a 40 mph gust, we only consider the crosswind induced by the helical vortex due to a gust-driven wind turbine wake. Any component of 40 mph gust itself is not included in the crosswind here. The contours for Runway 18-36 under the 40 mph (58.68 ft/s) gust wake are shown in Figures 3.7a and 3.7b. The rhombus area is a cross section of the area where the helical vortex exists (between the two red lines) and the area near the runway from south to north (between the two green lines). If we consider the crosswind above 12.1 mph (17.7 ft/s) as a high hazard, as shown in Table 2.1 from the literature, and below 12.1 as a low hazard, Figure 3.7b shows that a major portion of the runway is in the high hazard region.

The contours for Runway 18-36 under the 10 mph (14.67 ft/s) continuous wind speed condition, which is a mild wind condition, are shown in Figures 3.7c and 3.7d. Assuming that the 10 mph wind blows constantly, we calculated the summation of the crosswind induced by helical

vortex and generated by the 10 mph wind itself. Figure 3.7d shows that a partial area around the runway is within the high hazard region.

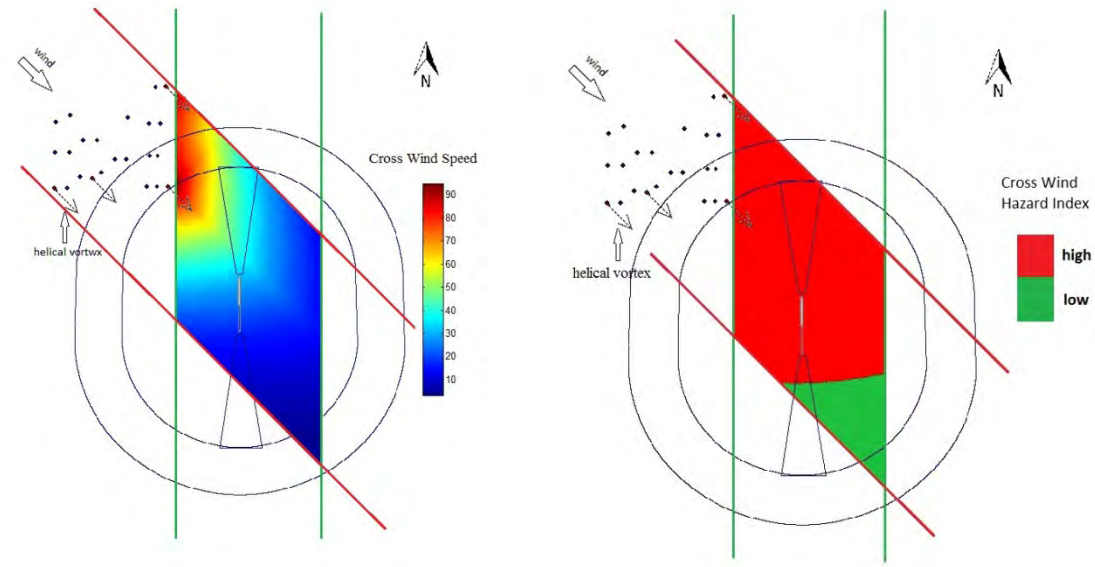

(a) Turbine wake induced crosswind under 40 mph gust (b) Hazard index under 40 mph gust

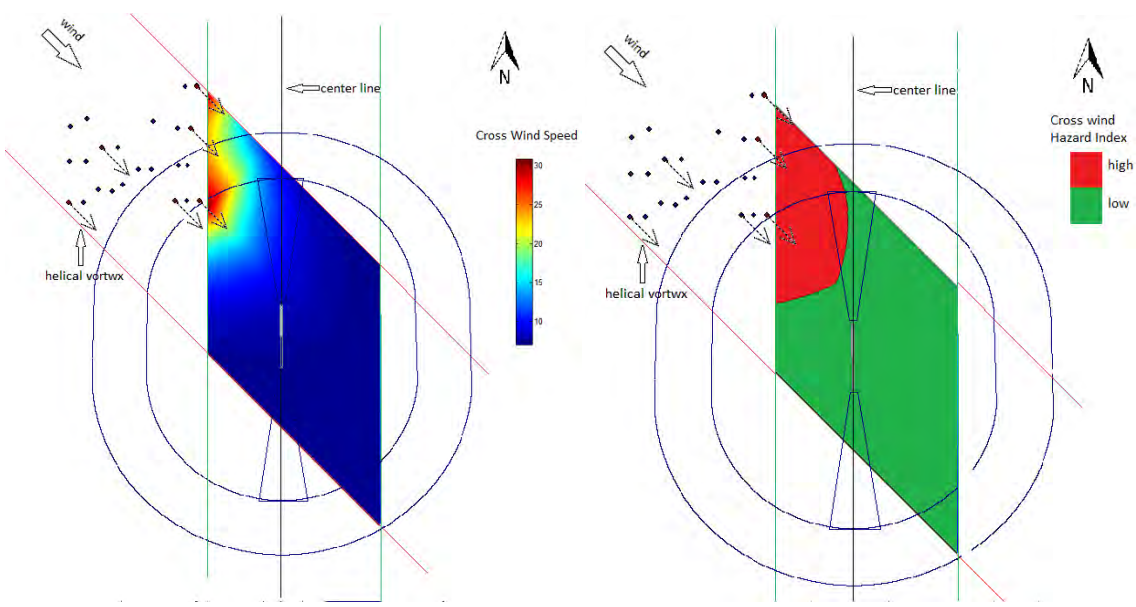

(c) Crosswind speed under 10 mph wind (d) Hazard index under 10 mph wind

FIGURE 3.7
Crosswind Speed and Hazard around the Rooks County Regional Airport

3.3 The Pratt Regional Airport Case

Figure 3.8 shows the aerial image and a sketch map of the Pratt Regional Airport. Runway 17-35 is the only open runway.

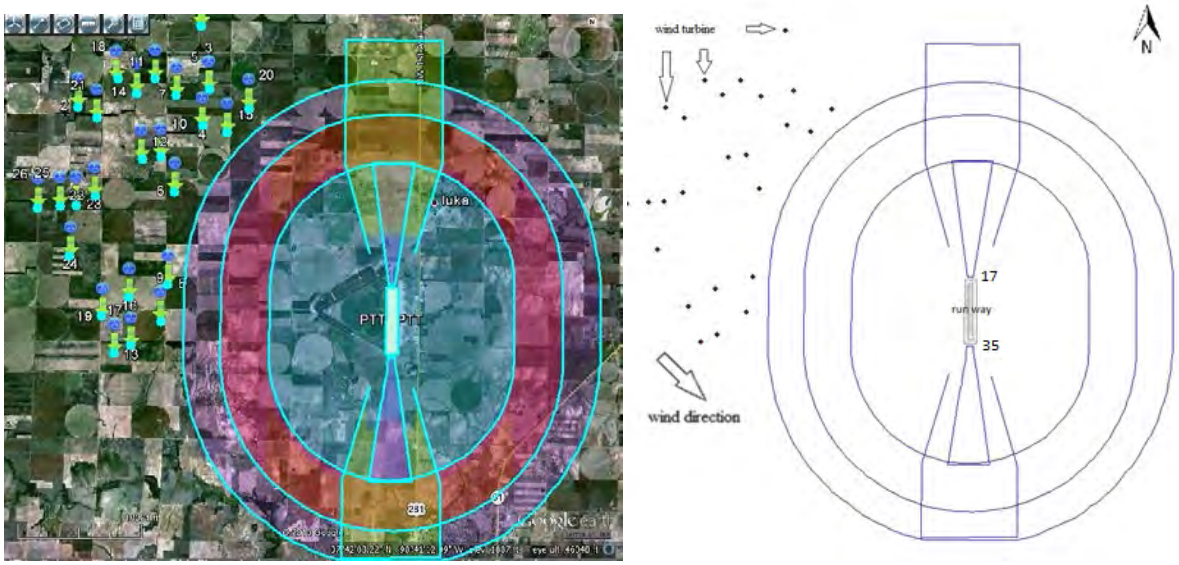

FIGURE 3.8
Pratt Regional Airport and Wind Farm with a Scenario of a Northwest Wind

3.3.1 The Roll Hazard Analysis

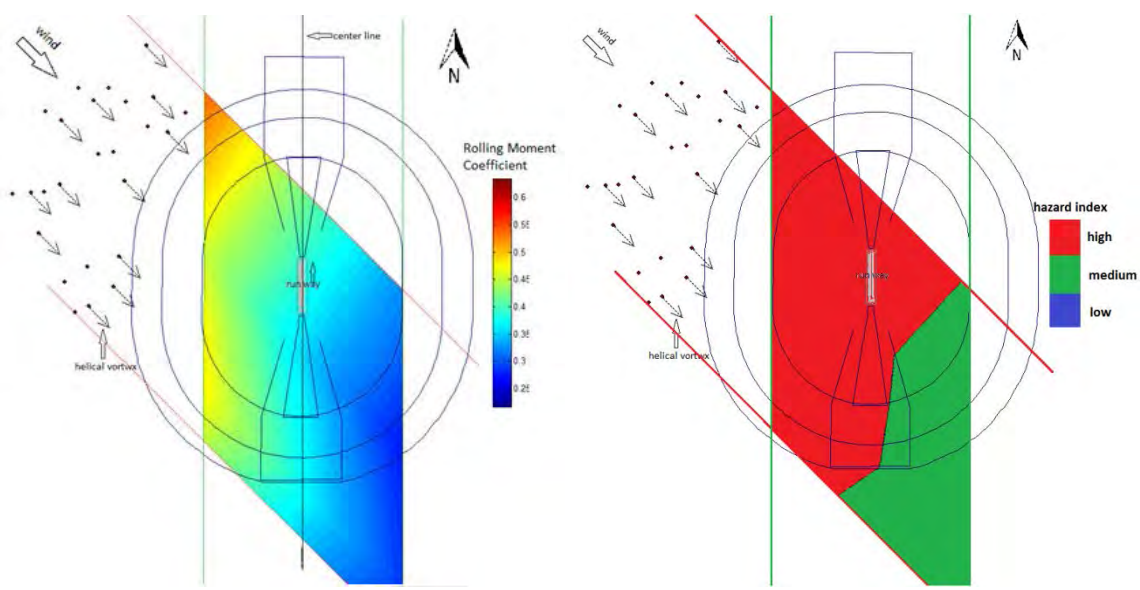

FIGURE 3.9
(a) Rolling Moment Coefficient and (b) Hazard Index around the Pratt Regional Airport

Based on this decay distribution in Appendix E, the rolling momentum coefficient can be calculated, and then the hazard index near the runway is determined. The contours for Runway 17-35 under the 40 mph wind speed condition are shown in Figure 3.9. Figure 3.9a shows the exact rolling moment value in the area, and Figure 3.9b shows the hazard index. As Figure 3.9b shows, the area around the runway is within the high hazard region.

Figure 3.10 is a plot of the end of Runway 17 and its approach surface from the airport layout plan drawing provided by KDOT. The approach surface is a 34:1 approach surface.

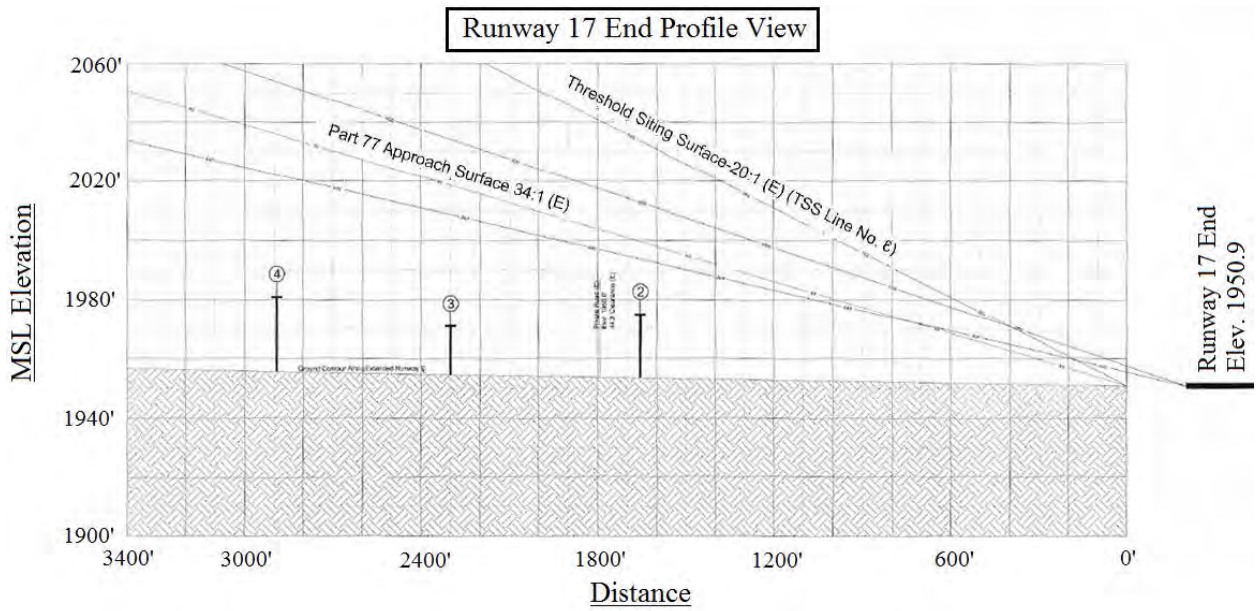

FIGURE 3.10
Approach Surface of Runway 17 in the Airport Layout Plan Drawing

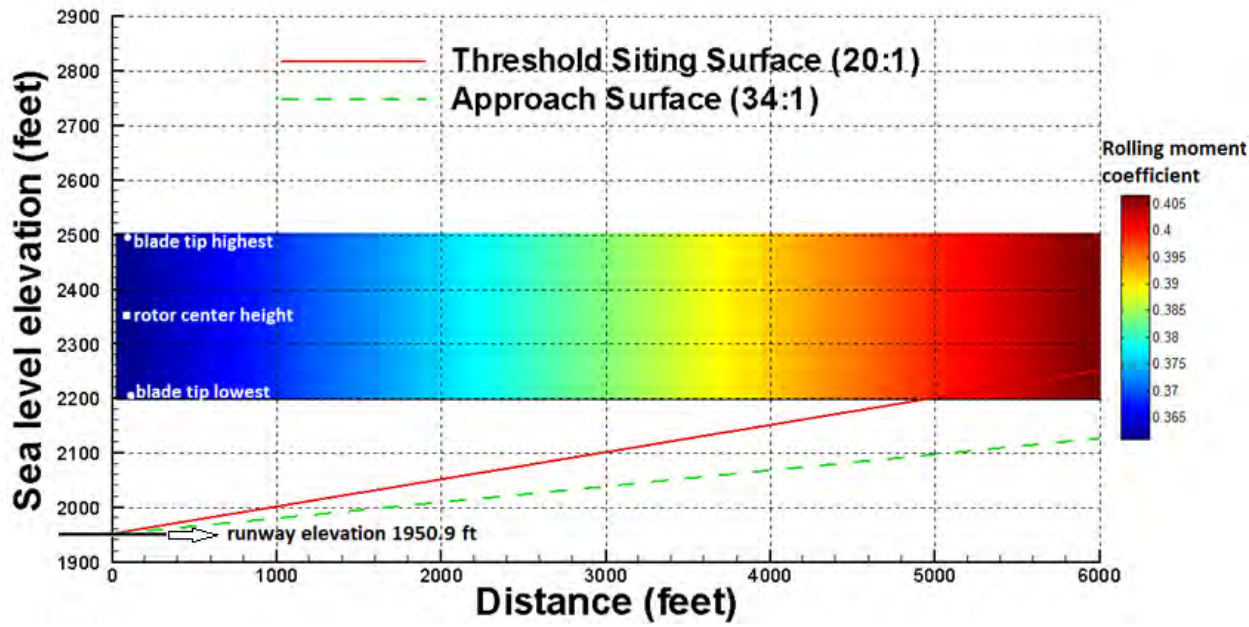

FIGURE 3.11
Rolling Moment Distribution along the Approach Surface of Runway 18 (All in the High Hazard Index Range)

We also extended the plot following the trend of the approaching surface and threshold siting surface and put the contours of rolling moment coefficient in Figure 3.11 for the elevation between 2200 ft and 2500 ft. The rolling moment coefficient along this runway and the extended trend up to 6000 ft (the limitation of the hazard area) distance is always in the high hazard range. The very end of the threshold site surface will experience the high hazard.

3.3.2 The Crosswind Hazard Analysis

Because the helical vortex can also enhance the crosswind acting on an airplane, we need to assess the crosswind hazard in the area around the runway in Pratt Regional Airport as well. Figure 3.12 shows the aerial image and a sketch map of Pratt Regional Airport. The crosswind direction to Runway 17-35 is from west to east.

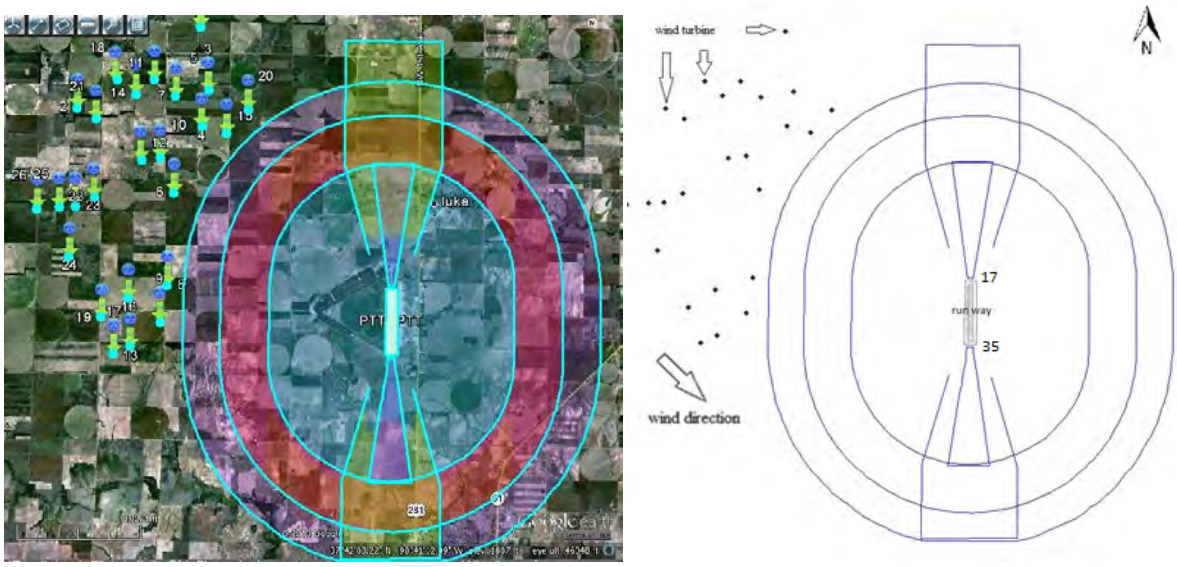

FIGURE 3.12
Pratt Regional Airport and Wind Farm with a Scenario of a Northwest Wind

Based on the same decay distribution in Appendix E, the crosswind speed and the hazard index near the runway can be calculated (see Appendix F).

Again, the case was analyzed in two scenarios: one is the 40 mph gust, and the other is the 10 mph continuous wind. The contours of the crosswind and the corresponding hazard for the 17-35 runway under the 40 mph (58.68 ft/s) wind speed condition are shown in Figures 3.13a and 3.13b. The rhombus colorful area is a cross section of the area where the helical vortex exists (between the two red lines) and the area near the runway from south to north (between the two green lines). If we consider the crosswind above 12.1 mph (17.7 ft/s) as a high hazard, as shown in Table 2.1 from the literature, and below 12.1 as a low hazard, Figure 3.13b shows that the runway is in the high hazard region.

The contours for Runway 17-35 under the 10 mph (14.67 ft/s) continuous wind speed condition, which is a mild wind condition, are shown in Figures 3.7c and 3.7d. Figure 3.13d shows that only a very small area around the runway near the wind turbines is within the high hazard region.

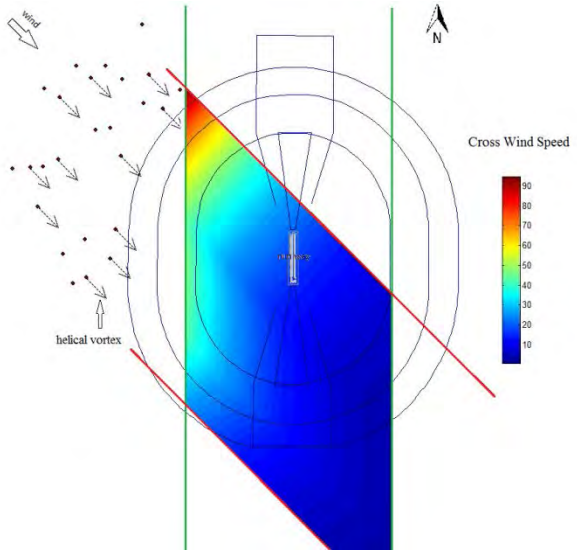

(a) Turbine wake induced crosswind under 40 mph gust

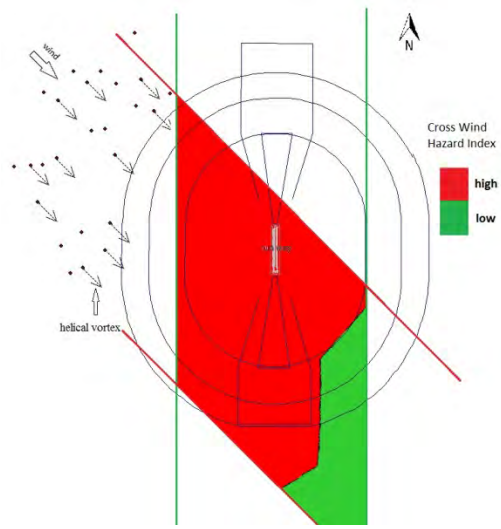

(b) Hazard index under 40 mph gust

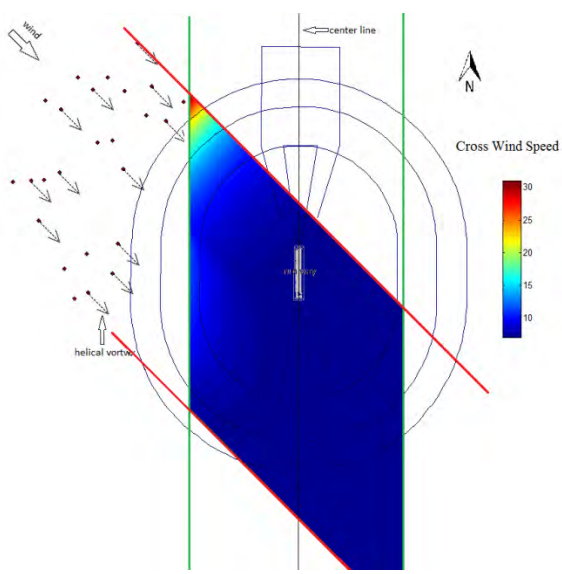

(c) Crosswind speed under 10 mph wind

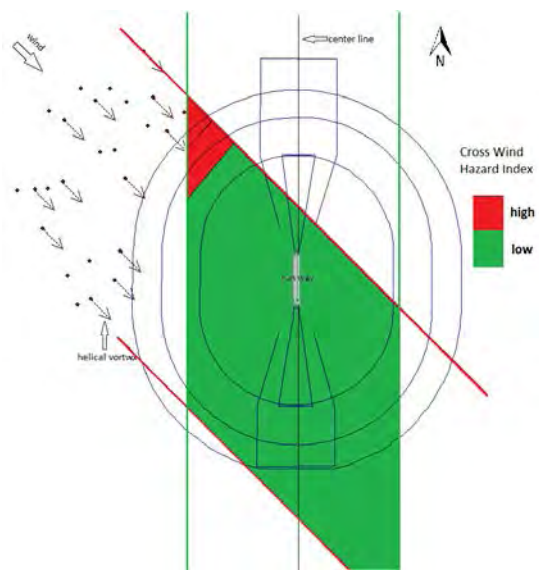

(d) Hazard index under 10 mph wind

FIGURE 3.13
Crosswind Speed and Hazard around the Pratt Regional Airport

Chapter 4: Conclusions and Recommendations

The literature review shows that wind farms may have an adverse impact on general aviation, in general, and more specifically with aircraft operating at or near an airport. The impacts of wind turbines on aviation include physical penetration of airspace, communication systems interferences and rotor blade-induced turbulence.

The results of this project support the findings in the literature search that the turbulence from a wind turbine can impact operations at a general aviation airport. Two case studies were used to illustrate the impact of turbulence from a wind turbine on a general aviation airport. This project analyzed the roll hazard and the crosswind hazard resulting from a wind farm located near a general aviation airport. The wind turbine wake model is based on a theoretical helical vortex model and the decay rate is calculated following the aircraft wake decay rate in the atmosphere.

The roll hazard analysis showed that for the Rooks County Regional Airport, the potential roll hazard index is in the high range as far out as 2.84 miles. For the Pratt Regional Airport, the roll hazard index is in the high range as far out as 1.14 miles. These numbers are based on a gust wind of 40 mph that is below the turbine brake wind speed of 55 mph. As the results show, the scenario is different according to the relative locations and orientations of the airport and the nearby wind farm. Therefore, the analysis has to be performed for each specific regional airport.

The crosswind hazard analysis for the Rooks County Regional Airport showed part of the airport in the high range even under the mild wind condition at 10 mph. The wind turbine wake increases the crosswind component to more than 12 mph which is considered high risk crosswind for small general aviation aircraft. For the Pratt Regional Airport, the crosswind hazard is relatively small under the mild wind condition (10 mph). When there is a gust of 40 mph wind, the turbine wake induced crosswind puts the majority of runway areas to high hazard areas at both of the airports.

It is recommended that additional studies should be performed to draw the proper correlation between the hazard index developed in this study and the safe operation of aircraft at low airspeeds and at low flight altitudes operating near or at a general aviation airport.

References

Air Safety Institute. *Operations at Nontowered Airports.* n.d. http://www.aopa.org/asf/publications/sa08.pdf. Accessed April 20, 2013.

AOPA. 2010. "Wind Turbines Can't Come at the Expense of Airports." http://www.aopa.org/News-and-Video/All-News/2010/July/8/Wind-turbines-cant-come-at-expense-of-airports.aspx. Accessed January 22, 2014.

Barrett, Stephen B. and Philip M. Devita. 2011. Transportation Research Board. "ACRP Synthesis 28: Investigating Safety Impacts of Energy Technologies on Airports and Aviation."

Brandon, John. 2012. "Recreationalflying.com." http://www.recreationalflying.com/tutorials/safety/wind_shear.html#definition. Accessed April 16, 2013.

Calleja, Jay. 2010. *National Agricultural Aviation Association*. http://www.agaviation.org/content/wind-energys-effect-farming. Accessed May 06, 2013.

Carbone, Giuseppe, and Luciano Afferrante. 2013. "A Novel Probabilistic Approach to Assess the Blade Throw Hazard of Wind Turbines." *Renewable Energy* 51: 474–481.

Civil Aviation Authority. 2011. "CAP 764: CAA Policy and Guidelines on Wind Turbines." London.

EMD International A/S. 2010. "Turbulence Impact Assessment: Hiiumaa Offshore Wind Farm, Estonia." Estonia.

Federal Aviation Administration. 2012. *Airport Design: Advisory Circular.* Washington, D. C: US DOT.

Graham, Howard. 2008. "Intimate Emptiness: The Flint Hills Wind Turbine Controversy." Master's Thesis, Lawrence.

Hardin, Jay C. 1982. "The Velocity Field Induced by a Helical Vortex Filament." *Physics of Fluids* 25: 1949–1952.

Horonjeff, Robert, X Francis McKelvey, J William Sproule, and B Seth Young. 2010. *Planning & Design of Airports (Fifth Edition).* McGraw Hill.

Knopper, Loren D, and Christopher A Ollson. 2011. *Health Effects and Wind Turbines: A Review of the Literature*. Ottawa ON, Canada: BioMed Central.

Meyers, J. and Meneveau, C. 2012. "Optimal Turbine Spacing in Fully Developed Wind Farm Boundary Layers." *Wind Energy* 15: 305–317. doi: 10.1002/we.469.

Mustakerov, Ivan, and Daniela Borissova. 2009. "Wind Turbines Type and Number Choice Using Combinatorial Optimization." *Renewable Energy* 35: 1887–1894.

Namowitz, Dan. 2012. " Wind Farms Could Be a Hazard to VFR Flights." http://www.aopa.org/News-and-Video/All-News/2012/February/23/Wind-farm-could-be-hazard-to-VFR-flights.aspx. Accessed January 22, 2014.

National Research Council. 2007. *Environmental Impacts of Wind-Energy Projects*. Washington, D.C.: The National Academies Press.

NationAir Aviation Insurance. 2012. www.nationair.com.

Pohl, Johannes, Gundula Hubner, and Anja Mohs. 2012. "Acceptance and Stress Effects of Aircraft Obstruction Markings of Wind Turbines." *Energy Policy* 50: 592–600.

Slattery, Micheal C., Eric Lantz, and Becky L. Johnson. 2011. "State and Local Economic Impacts from Wind Energy Projects: Texas Case Study." *Energy Policy* 39: 7930–7940.

Sarpkaya T., R.E. Robins, and D.P. Delisi. 2001. "Wake-Vortex Eddy-Dissipation Model Predictions Compared with Observations." *Journal of Aircraft* 38 (4): 687–692. doi:10.2514/2.2820.

Stoevesandt, Bernhard. 2012. " Wind Farms: A Danger to Ultra-Light Aircraft?" http://www.eurekalert.org/pub_releases/2012-08/f-wfa081312.php. Accessed January 22, 2014.

Stump, Brad. 2012. "Wind Farm Developments and the Potential Impact on Aviation in Dekalb County, IN." http://www.co.dekalb.in.us/egov/docs/13576689114438.pdf

Twombly, Ian J. 2009. " Wind Turbines Represent Potential Hazard to Pilots." http://www.aopa.org/News-and-Video/All-News/2009/March/26/Wind-turbines-represent-potential-hazard-to-pilots.aspx. Accessed January 22, 2014.

www.energybible.com. 2012. www.energybible.com/wind_energy/wind_speed. Accessed April 11, 2013.

Yang, Zifeng, Partha Sarkar, Hui Hu. 2012. "Visualization of the Tip Vortices in a Wind Turbine Wake." *Journal of Visualization* 15:39–44.

Zheng, Z. C., Ying Xu. 2008. "*A Visualized Wake Hazard Assessment*." 46th AIAA Aerospace Sciences Meeting and Exhibit, January 7–10, Reno, Nevada.

Zheng, Z. C., Ying Xu, D. K. Wilson. 2009. "*Behaviors of Vortex Wake in Random Atmospheric Turbulence*." *Journal of Aircraft* 46 (6): 2139–2144. doi:10.2514/1.44288.

www.aweo.org/windmodels

Appendix A: Wind Turbine Wake Vortex Circulation

The experimental study referenced in this report was conducted in an aerodynamic/atmospheric boundary layer (AABL) wind tunnel located at Iowa State University as shown in Figure A.1 (Yang et al. 2012). This experiment was to simulate a radius of 45 m wind turbine using a 1:350 scale down small turbine. During the experiments, the wind speed at the hub height was set to be 4.0 m/s (i.e., U_0=4.0 m/s). The corresponding chord Reynolds number (i.e., based on the averaged chord length of the rotor blades and the wind speed at hub height) would be about 6,000, which is significantly lower than those of real wind turbines. The chord Reynolds number would have significant effects on the characteristics of wind turbine performance. However, the fundamental behavior of the helical tip vortices and turbulent wake flow structures at the downstream of wind turbines would be almost independent to the chord Reynolds number. The wind turbines with similar tip-speed-ratio (TSR) would produce similar near wake characteristics such as helical shape, rotation and tip vortices.

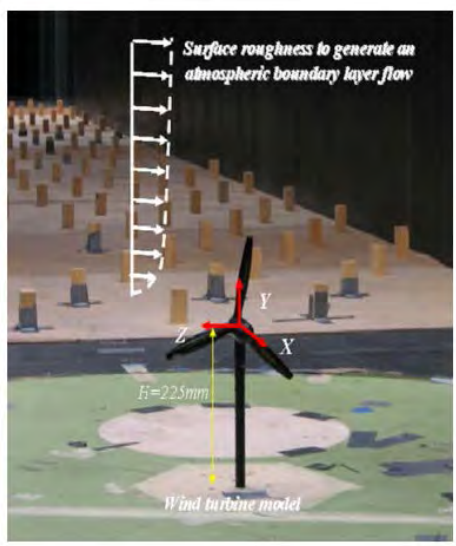

(Source: Yang, et al. 2012)

FIGURE A.1
Model of a Turbine in a Wind Tunnel Experiment

It is therefore reasonable using the data in Yang at el. (2012) to scale up the rotation based on the incoming wind speed and the dimension of the large wind turbine.

In that paper, V_0 = 4 m/s and the rotor diameter is 0.254 m and the vorticity and velocity result is shown in Figure A.2. Using the maximum of the velocity value and the area of vortex the circulation can be calculated:

$$\Gamma = 2\pi rv = 2\pi \times 0.01\text{m} \times (4(\text{m/s}) * 1.15) = 0.289\ \text{m}^2/\text{s}$$

We thus can calculate the circulation in our case as:

$$\Gamma = 0.289(\frac{\text{m}^2}{\text{s}}) \times \left(\frac{17.88(\frac{\text{m}}{\text{s}})}{4\left(\frac{\text{m}}{\text{s}}\right)}\right) \times \left(\frac{91.44\text{m}}{0.254\text{m}}\right) = 465.1\frac{\text{m}^2}{\text{s}} = 5006.3\frac{ft^2}{s}$$

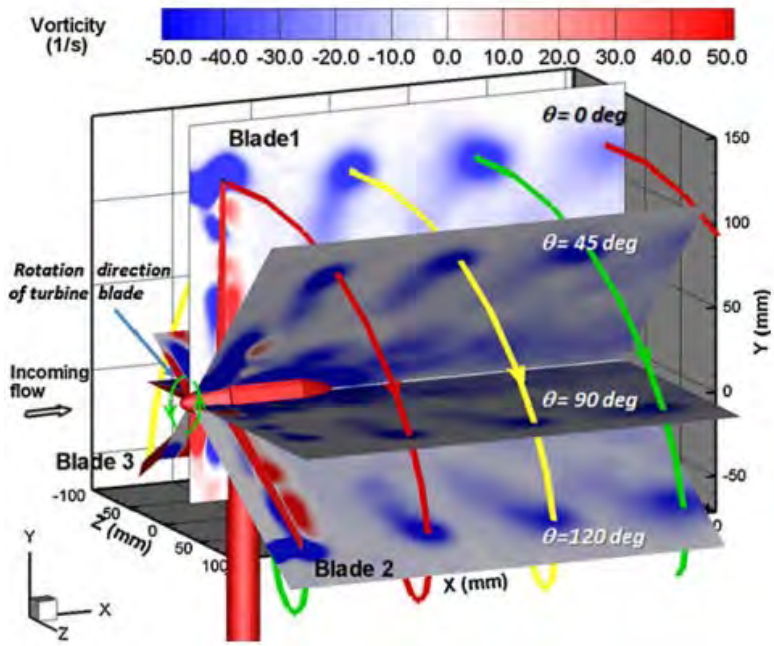

(a) Vorticity result

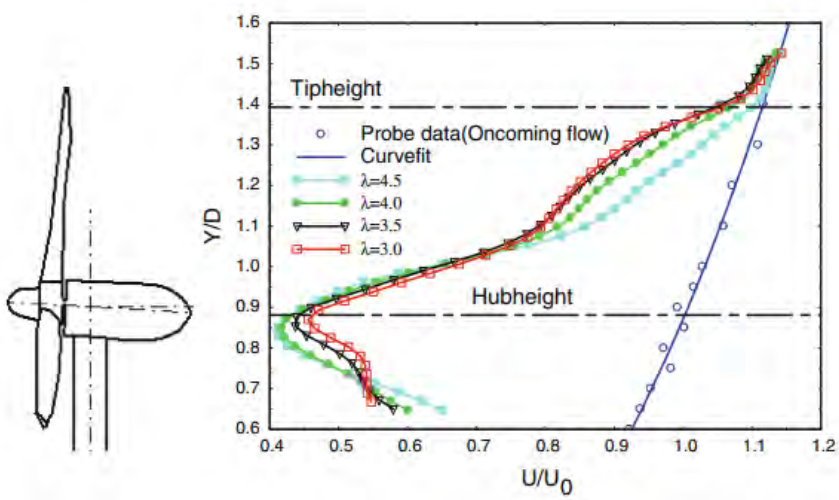

(b) Velocity result

(Source: Yang et al. 2012)

FIGURE A.2
Vorticity and Velocity Distribution

Appendix B: Helical Vortex Model for Wind Turbine Vortex Wake

Wind turbine wakes are modeled by helical vortices (Hardin 1982). In a Cartesian coordinate, when the radius is less than the helical radius ($r < R_{helical}$):

$$u_r = \frac{\Gamma_{helical} R_{helical}}{\pi k^2} S_2$$
$$u_\phi = \frac{\Gamma_{helical} R_{helical}}{r \pi k} S_1$$
$$w = \frac{\Gamma_{helical}}{2\pi k} - \frac{\Gamma_{helical} R_{helical}}{\pi k^2} S_1$$

where $\Gamma_{helical}$ is the circulation of the vortex filament, $R_{helical}$ is the radius of the helical vortex, and:

$$S_1(r,\phi) = \sum_{m=1}^{\infty} m K'_m \left(\frac{R_{helical} m}{k} \right) I_m \left(\frac{rm}{k} \right) \cos(m\psi)$$
$$S_2(r,\phi) = \sum_{m=1}^{\infty} m K'_m \left(\frac{R_{helical} m}{k} \right) I'_m \left(\frac{rm}{k} \right) \sin(m\psi)$$

$$\psi = \phi - z / k$$

where K'_m and I_m are modified Bessel functions of the *m*th order.

When the radius is greater than the helical radius ($r > R_{helical}$):

$$u_r = \frac{\Gamma_{helical} R_{helical}}{\pi k^2} S_4$$
$$u_\phi = \frac{\Gamma_{helical}}{2\pi r} + \frac{\Gamma_{helical} R_{helical}}{r \pi k} S_3$$
$$w = -\frac{\Gamma_{helical} R_{helical}}{\pi k^2} S_3$$

where:

$$S_3(r,\phi) = \sum_{m=1}^{\infty} m K_m \left(\frac{rm}{k} \right) I'_m \left(\frac{R_{helical} m}{k} \right) \cos(m\psi)$$
$$S_4(r,\phi) = \sum_{m=1}^{\infty} m K'_m \left(\frac{rm}{k} \right) I'_m \left(\frac{R_{helical} m}{k} \right) \sin(m\psi)$$

Appendix C: Rolling Moment Coefficient Calculation

Since we have the wind turbine wake velocity field from the helical vortex model, we can calculate the induced rolling moment coefficient on an aircraft that flies through the wake (Zheng and Xu 2008). Considering the aircraft with a wing span of $2s_F$ and flying speed W_F, we have, for the lift force acting on a spanwise element section dx_F:

$$\boldsymbol{\rho W_F \Gamma_F(x_F) dx_F = \frac{1}{2} \rho W_F{}^2 C_{LF}(x_F)\, dx_F \cdot c_F(x_F)} \qquad \textbf{Equation C.1}$$

where Γ_F is the circulation, C_{LF} is the lift coefficient, and $c_F(x_F)$ is the chord length of the aircraft at x_F. Assuming that $\partial C_{LF}/\partial\alpha$ is approximately constant in the range of angle of attack α, we have:

$$\boldsymbol{\Gamma_F(x_F) = \frac{\frac{1}{2} W_F \Delta\alpha \cdot \partial C_{LF}}{\partial\alpha}\; c_F(x_F)} \qquad \textbf{Equation C.2}$$

Since

$$\boldsymbol{\Delta\alpha \approx \frac{\nu}{W_F}} \qquad \textbf{Equation C.3}$$

where ν is the vertical velocity component at the location of the wing (produced by the wake vortex system). We have

$$\boldsymbol{\Gamma_F(x_F) = \frac{1}{2} v(x_F) \frac{\partial C_{LF}}{\partial\alpha}\; c_F(x_F)} \qquad \textbf{Equation C.4}$$

The rolling moment on the wing can then be expressed by:

$$M_{RF} = \int_{-s_F}^{s_F} \rho W_F \Gamma_F(x_F) x_F dx_F = \frac{1}{2}\rho W_F \frac{\partial C_{LF}}{\partial \alpha} \int_{-s_F}^{s_F} v(x_F)\, c_F(x_F)\, x_F dx_F$$ **Equation C.5**

And the rolling moment coefficient is:

$$C_{RF} = \frac{M_{RF}}{\frac{1}{2}\rho W_F{}^2 S_F \cdot 2s_F} = \frac{\partial C_{LF}}{\partial \alpha} \cdot \frac{1}{2S_F \cdot 2s_F} \int_{-s_F}^{s_F} v(x_F)\, c_F(x_F) x_F dx_F$$ **Equation C.6**

where S_F is the plan form area and is defined as

$$S_F = 2s_F \bar{c}_F$$ **Equation C.7**

with $\bar{c}_F$ equal to the average chord length of the wing.

Using a Fourier series, we define

$$\Gamma_F(\theta) = 4s_F W_F [\frac{P_0}{2} + \sum_1^N (P_0 cos2n\theta + Q_n sin2n\theta)]$$ **Equation C.8**

where θ is used to replace the spanwise coordinate of the airplane wing x_F, defined as:

$$cos\theta = -x_F/s_F. \; -1 \leq x_F/s_F \leq 1 \; for \; 0 \leq \theta \leq \pi$$ **Equation C.9**

Then from the first part of Equation C.6, the rolling moment coefficient can be expressed as

$$C_{RF} = \frac{4s_F{}^2}{S_F} \int_0^{\pi} [\frac{P_0}{2} + \sum_1^N (P_n cos2n\theta + Q_n sin2n\theta)]\,(-cos\,\theta)(-sin\theta) d\theta$$

$$= \pi/4\,(AR)_F Q_1$$ **Equation C.10**

where $(\mathrm{AR})_F$ is the aspect ratio of the wing. Now with Equations C.4 and C.8, we have

$$\frac{\boldsymbol{v}(\boldsymbol{x_F})}{\boldsymbol{W_F}} = \frac{\mathbf{2}\boldsymbol{\Gamma_F}(\boldsymbol{x_F})}{\boldsymbol{W_F}\frac{\partial \mathbf{C_{LF}}}{\partial \boldsymbol{\alpha}}\ \boldsymbol{c_F}(\boldsymbol{x_F})} = \frac{\mathbf{4}\ (\boldsymbol{AR})_{\boldsymbol{F}}}{\frac{\partial \mathbf{C_{LF}}}{\partial \boldsymbol{\alpha}}\frac{\boldsymbol{c_F}^{(6)}}{\bar{\boldsymbol{c}}_{\boldsymbol{F}}}}[\frac{\boldsymbol{P_0}}{\mathbf{2}} + \sum_{\mathbf{1}}^{\boldsymbol{N}}(\boldsymbol{P_n cos2n\theta} + \boldsymbol{Q_n sin2n\theta})]$$

$$= [\frac{\boldsymbol{A_0}}{\mathbf{2}} + \sum_{\mathbf{1}}^{\boldsymbol{N}}(\boldsymbol{A_n cos2n\theta} + \boldsymbol{B_n sin2n\theta})]\frac{\bar{\boldsymbol{c}}_{\boldsymbol{F}}}{\boldsymbol{c_F}(\boldsymbol{\theta})} \qquad \textbf{Equation C.11}$$

for

$$\boldsymbol{A_n} = \frac{\mathbf{4}\ (\boldsymbol{AR})_{\boldsymbol{F}}}{\frac{\partial \mathbf{C_{LF}}}{\partial \boldsymbol{\alpha}}}\boldsymbol{P_n} \qquad \textbf{Equation C.12}$$

and

$$\boldsymbol{B_n} = \frac{\mathbf{4}\ (\boldsymbol{AR})_{\boldsymbol{F}}}{\frac{\partial \mathbf{C_{LF}}}{\partial \boldsymbol{\alpha}}}\boldsymbol{Q_n} \qquad \textbf{Equation C.13}$$

Hence, with Equation C.10

$$\boldsymbol{C_{RF}} = \frac{\boldsymbol{\pi}}{\mathbf{16}}\frac{\partial \mathbf{C_{LF}}}{\partial \boldsymbol{\alpha}}\boldsymbol{B_1} \qquad \textbf{Equation C.14}$$

From Equation C.11 we can see that

$$\frac{\boldsymbol{A_0}}{\mathbf{2}} + \sum_{\mathbf{1}}^{\boldsymbol{N}}(\boldsymbol{A_n cos2n\theta} + \boldsymbol{B_n sin2n\theta}) = \frac{\boldsymbol{v}(\boldsymbol{\theta})\ \boldsymbol{c_F}(\boldsymbol{\theta})}{\boldsymbol{W_F}\bar{\boldsymbol{c}}_{\boldsymbol{F}}} \qquad \textbf{Equation C.15}$$

That is, if we perform a Fourier series expansion on $\frac{v(\theta)\, c_F(\theta)}{W_F \bar{c}_F}$, only the first coefficient of the sine series of that series is needed to calculate the rolling moment coefficient.

If we let

$$\boldsymbol{F(\theta) = \frac{v(\theta)\, c_F(\theta)}{W_F \bar{c}_F}}$$ **Equation C.16**

then

$$\boldsymbol{C_{RF} = \frac{\pi}{16} \frac{\partial C_{LF}}{\partial \alpha} \frac{\pi}{2} \int_0^{\pi} F(\theta) \sin(2\theta) d\theta}$$ **Equation C.17**

where C_{LF} is the lift coefficient, α is the angle of attack. In our case, $\frac{\partial C_{LF}}{\partial \alpha}$ equals to 0.075/degree, 4.2972 /rad. In addition, θ can be determined by x_F, the position of each section, and s_F the length of the wing. $\cos(\theta) = -\frac{x_F}{s_F}$

where $v(\theta)$ is the vertical velocity, $c_F(\theta)$ is the chord length, $\overline{c_F}$ is the average chord length, W_F is the flying speed, for our case, its 80 m/s. And

$$\frac{c_F(\theta)}{\overline{c_F}} = \frac{20}{13}(1 - 0.7\,|\frac{x_F}{s_F}|) = \frac{20}{13}(1 - 0.7\,|\cos(\theta)|)$$ **Equation C.18**

Appendix D: Roll Hazard Index

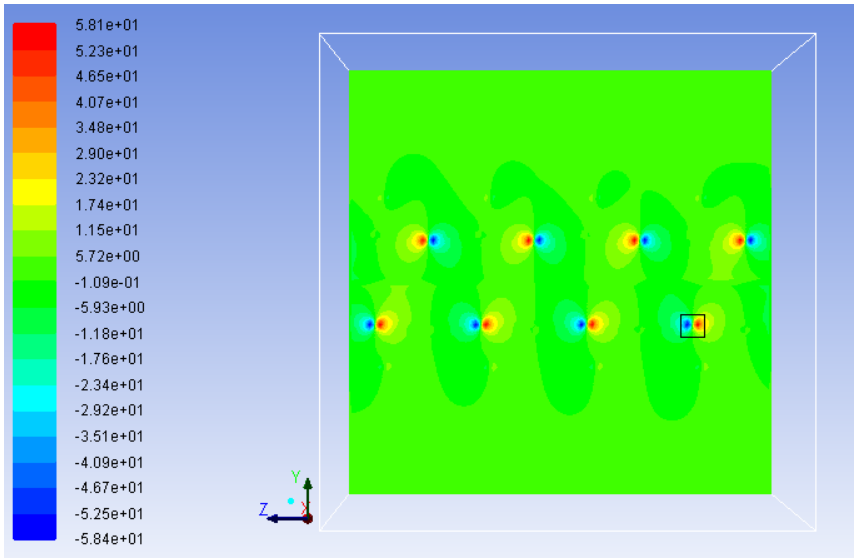

FIGURE D.1
Y-Direction Velocity on the Center X-Z Cutting Plane

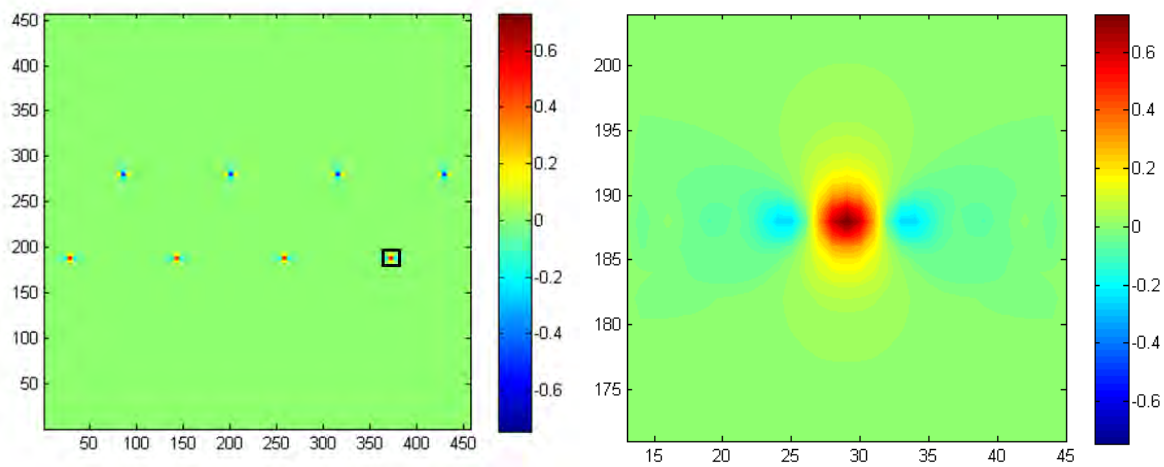

FIGURE D.2
(a) The Rolling Momentum Coefficient in the Domain and (b) in the Zoom-In Domain

In order to evaluate the roll hazard caused by the wind turbine wake, the induced rolling moment coefficient on a wake-penetrating aircraft is calculated based on the vertical component velocity distribution. Figure D.1 shows the y-direction velocity on a cutting plane. With the y-direction velocity, we can calculate the rolling moment coefficient using the relations developed in Appendix C. Figure D.2a is the resultant rolling momentum coefficient acting on a 30-ft

wingspan airplane when it is passing through the turbine wake region. The highest rolling momentum coefficient occurs at the center of the helical vortex core, which can be seen in Figure D.2b in a zoom-in region.

The relative magnitude between the operable rolling moment and the rolling moment induced by the wind turbine wake is used in this study to determine the hazard index.

The rolling moment coefficient that the airplane is able to operate is modeled by this formula:

$$C_R = 2C_{l\delta_A}\delta_A;$$

For a normal airplane

$$0 < C_{l\delta_A} < 0.4$$

$$0 < \delta_A < 20°$$

So at the maximum:

$$C_R = 2C_{l\delta_A}\delta_A = 2 \times 0.4 \times \frac{20}{180} \times \pi = 0.28$$

Appendix E: Rolling Moment Coefficient Decay with Distance

The local circulation Γ_i can be calculated by the initial circulation Γ_0 and vortex span b_0 after time t (Zheng et al. 2009):

$$\frac{\Gamma_i}{\Gamma_0} = \exp\left(-C\frac{t\Gamma_0}{2\pi {b_0}^2 {T_c}^*}\right) \qquad \textbf{Equation E.1}$$

where C is a constant of 0.45, and ${T_c}^*$ is determined by the following calculation:

$$\varepsilon^* = \frac{2\pi b_0}{\Gamma_0}(\varepsilon b_0)^{1/3} \qquad \textbf{Equation E.2}$$

For a high turbulence case at the turbulent intensity 10%, ε is 0.01 in our case, which indicates that ε^* has a high value and the eddy-dissipation rate in the entire range can be approximately related by this formula:

$$\varepsilon^*({T_c}^*)^{4/3} = 0.7475 \qquad \textbf{Equation E.3}$$

So

$${T_c}^* = \left(\frac{0.7475}{\varepsilon^*}\right)^{3/4} = \left(\frac{0.7475\Gamma_0}{2\pi b_0(\varepsilon b_0)^{1/3}}\right)^{3/4} \qquad \textbf{Equation E.4}$$

$$\frac{\Gamma_i}{\Gamma_0} = \exp\left(-C\frac{t\Gamma_0}{2\pi {b_0}^2\left(\frac{0.7475\Gamma_0}{2\pi b_0(\varepsilon b_0)^{\frac{1}{3}}}\right)^{\frac{3}{4}}}\right) = \exp\left(\frac{-Ct(\varepsilon\Gamma_0)^{1/4}}{0.956(\pi)^{1/4}b_0}\right) \qquad \textbf{Equation E.5}$$

At distance S with the wind speed V_0

$$t = \frac{S}{V_0}$$ **Equation E.6**

$$\frac{\Gamma_i}{\Gamma_0} = \exp\left(\frac{-CS(\varepsilon\Gamma_0)^{0.25}}{1.2727 V_0 b_0}\right)$$ **Equation E.7**

For the 18-36 runway of Rooks County Regional Airport under the northwest wind situation, the maximum induced rolling moment coefficient on the 30-ft wingspan GA aircraft caused by a wind turbine is 0.65, when the wake is close to the wind turbine. The induced rolling moment coefficient decays with distance due to atmospheric turbulence, as shown in Figure E.1. At lower wind speeds, the induced rolling moment coefficient becomes lower, and when the distance from the wind turbine increases, the coefficient value becomes lower.

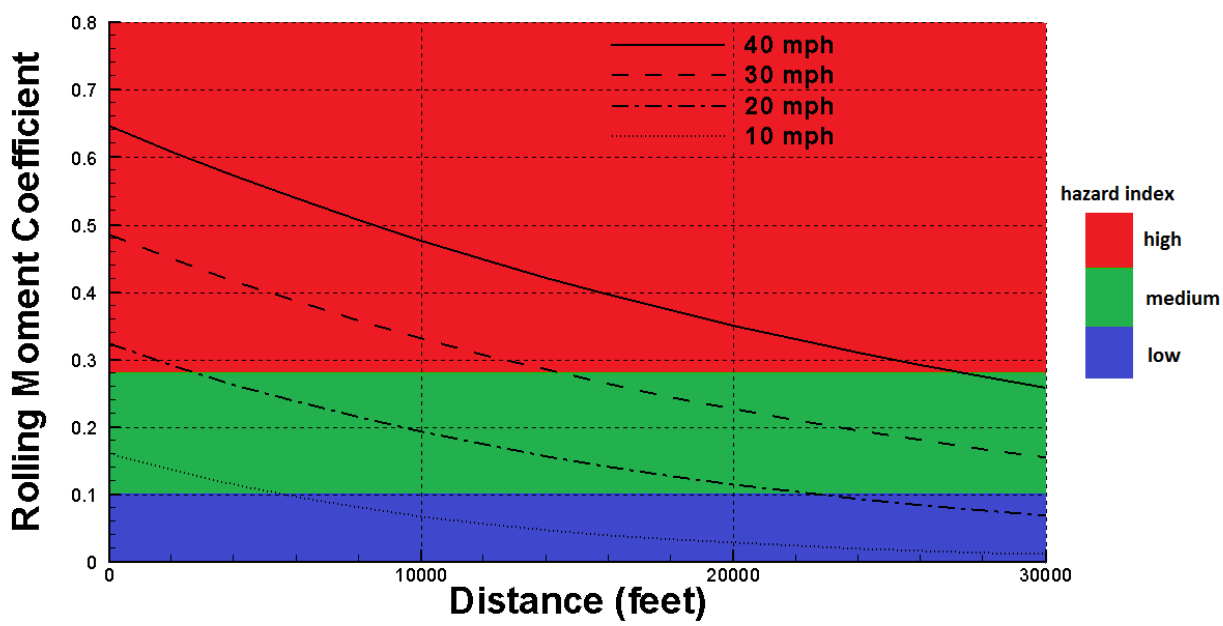

FIGURE E.1
Rolling Moment Coefficient Decay with Distance

For the 17-35 runway of Pratt Regional Airport under the northwest wind situation, the maximum induced rolling moment coefficient on the 30-ft wingspan GA aircraft caused by a wind turbine is 0.65, when the wake is close to the wind turbine. The induced rolling moment coefficient decays with distance due to atmospheric turbulence, as shown in Figure E.2. At lower wind speeds, the induced rolling moment coefficient becomes lower, and when the distance from the wind turbine increases, the coefficient value becomes lower.

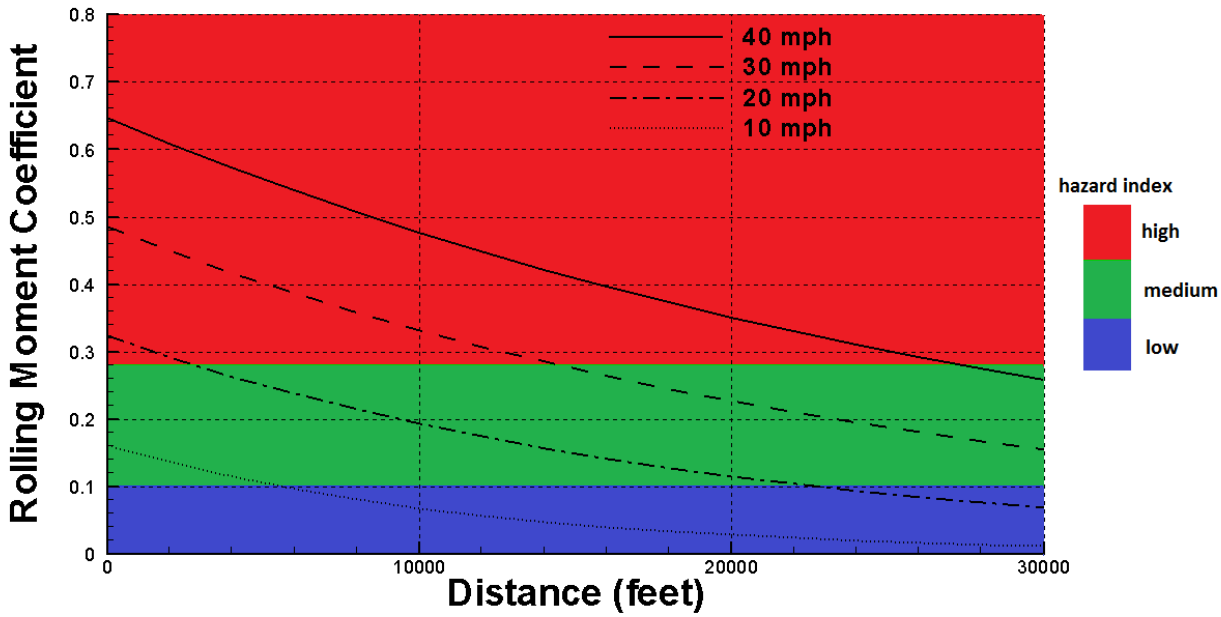

FIGURE E.2
Rolling Moment Coefficient Decay with Distance

Appendix F: Crosswind from Wind Turbine Wake on an Airplane

Figure F.1 shows the 45 degree direction velocity which is vertical to the aircraft body on a cutting plane parallel to the ground shown in Figure F.2. The maximum velocity from the turbine wake is 95.25 mph (139.7 ft/s).

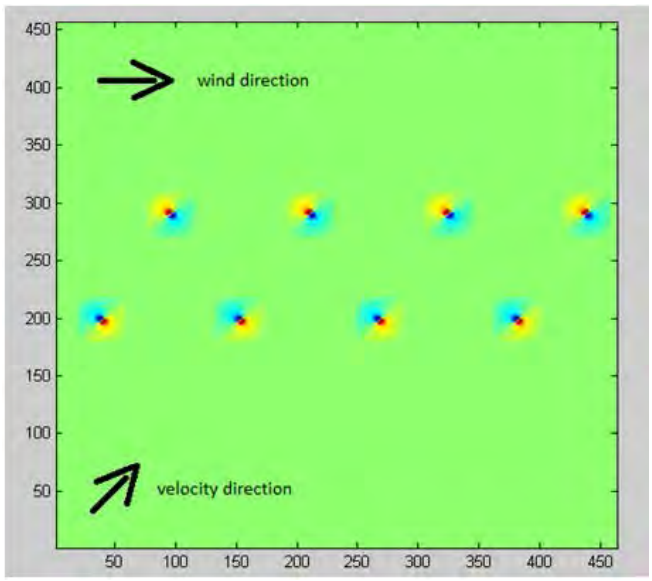

FIGURE F.1
45 Degree Direction Velocity Value from the Wind Turbine Wake on a Cutting Plane

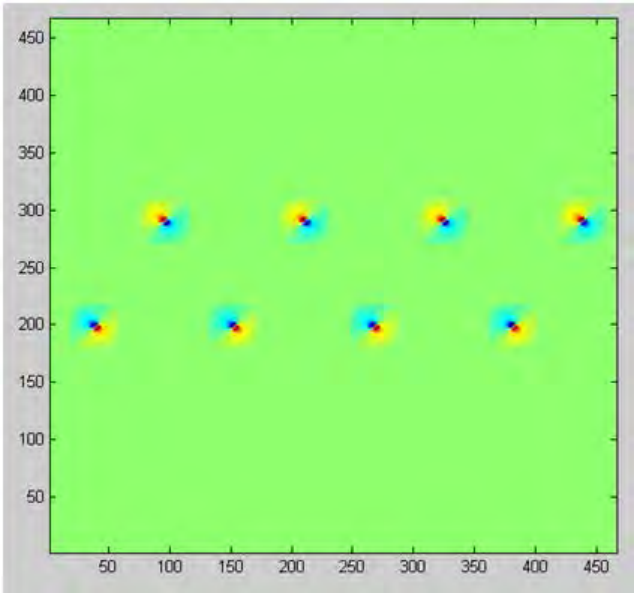

FIGURE F.2
45 Degree Direction Velocity Value Added by the Background Velocity

The value of background wind component on crosswind direction is the wind speed 40 mph multiplied by cosine 45 degree equal to 28.28 m ph ($40\,mph \times \frac{\sqrt{2}}{2} = 28.28\,mph = 41.48\,ft/s$). If we add this value to the velocity field in Figure F.1, it is what Figure F.2 shows. The maximum velocity is 123.53 mph (181.18 ft/s)

TABLE F.1
Possible Maximum Crosswind Velocity in the Wind Turbine Wake in Different Background Wind Speeds

Wind speed (mph)	40	30	20	10
Cross wind component (mph)	28.28	21.21	14.14	7.07
Max vortex induced cross wind (mph)	95.25	71.44	47.63	23.81
Max crosswind velocity (mph)	123.53	92.65	61.77	30.88

The limit, as shown in Table 2.1 in the literature, is 10.5 knot which is 12.1 mph (17.7 ft/s). Table F.1 lists the maximum crosswind velocity in different background wind speeds. If the wind is larger than 20 mph, the wind component at cross direction is already over the 12 mph limit. So we consider the 10 mph wind speed as an example to see the hazard in the airport.

K-TRAN

KANSAS TRANSPORTATION RESEARCH AND NEW-DEVELOPMENT PROGRAM

AD ASTRA PER ASPERA

Kansas
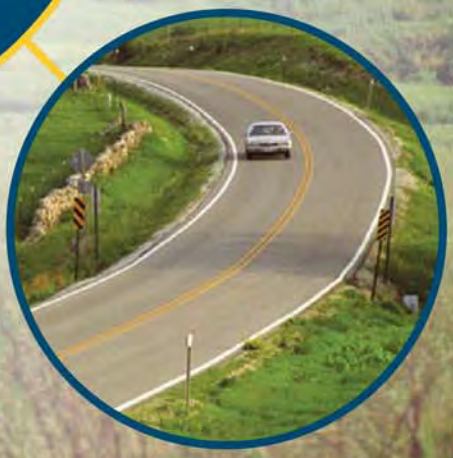
Department of Transportation